

Urban aerosol radiative properties: Measurements during the 1999 Atlanta Supersite Experiment

Christian M. Carrico,¹ Michael H. Bergin, and Jin Xu

School of Civil and Environmental Engineering, Georgia Institute of Technology, Atlanta, Georgia, USA

Karsten Baumann

School of Earth and Atmospheric Sciences, Georgia Institute of Technology, Atlanta, Georgia, USA

Hal Maring

Rosentiel School for Marine and Atmospheric Science, University of Miami, Miami, Florida, USA

Received 25 July 2001; revised 30 April 2002; accepted 12 June 2002; published 6 February 2003.

[1] As part of the Atlanta Supersite 1999 study, aerosol radiative and related physical and chemical properties are examined on the basis of measurements of PM_{2.5} (aerosol particles with aerodynamic diameters, D_p , less than 2.5 μm) in urban Atlanta. In addition to potential compliance issues with proposed regulatory standards, PM_{2.5} concentrations in Atlanta and the surrounding region are large enough to have an important impact on atmospheric radiative transfer and hence visibility and potentially regional climate. Arithmetic means and standard deviations of the light scattering by PM_{2.5} (σ_{sp} at 530 nm) and absorption coefficients (σ_{ap} at 550 nm) measured at a controlled relative humidity of $49 \pm 5\%$ are 121 ± 48 and $16 \pm 12 \text{ Mm}^{-1}$, respectively. Though the mean light extinction coefficient (σ_{ep}) in Atlanta is much larger than background sites, it is comparable to nonurban areas in the interior southeast United States highlighting the contribution of a regional haze here. The single scattering albedo (ω_0) in Atlanta is 0.87 ± 0.08 and is $\sim 10\%$ lower than reported in nonurban polluted sites, likely a result of the emission of elemental carbon (EC) from mobile sources. A pronounced diel pattern in aerosol properties is observed with clear influences from mobile sources (morning rush hour maxima in concentrations, particularly soot-related indicators) and atmospheric mixing (afternoon minima). A strong linear relationship between σ_{sp} and PM_{2.5} is observed, and using several techniques, gives a range of mean mass scattering efficiencies (E_{sp}) from $= 3.5$ to $4.4 \text{ m}^2 \text{ g}^{-1}$. EC and σ_{ap} are observed to have a relationship though less strongly correlated than σ_{sp} and PM_{2.5}. Four methods of determining the mass absorption efficiency of EC give E_{ap} ranging from 5.3 to $18.3 \text{ m}^2 \text{ g}^{-1}$. This wide range of values is a result of the variability in aerosol properties, uncertainties in the light absorption method, and in particular, differences in the EC measurement techniques. Best agreement was found using measured EC mass distributions using a multistage impactor in comparison to σ_{ap} calculated with a Mie code yielding $E_{\text{ap}} = 9.5 \pm 1.5 \text{ m}^2 \text{ g}^{-1}$, while EC mass summed from the impactor stages in comparison to measured σ_{ap} gives $E_{\text{ap}} = 9.3 \pm 3.2 \text{ m}^2 \text{ g}^{-1}$. Mie light-scattering calculations using inputs of measured mass and EC size distributions give geometric mean light scattering and absorption $D_p = 0.54$ and $0.13 \mu\text{m}$, respectively, and show the dominance of the submicrometer diameter particles to light extinction in the urban environment. Based on the measured aerosol optical depth in Atlanta, $\delta_a(500 \text{ nm}) = 0.44 \pm 0.22$, and other radiative measurements, a best estimate of the average direct aerosol radiative forcing at the top of the atmosphere (a measure of the climate significance) is $\Delta F = -11 \pm 6 \text{ W m}^{-2}$ in Atlanta. This value is an order of magnitude greater than global mean estimates for aerosols underscoring the influence of aerosol particles on radiative transfer in the urban environment. *INDEX TERMS:* 0305 Atmospheric Composition and Structure: Aerosols and particles (0345, 4801); 0394 Atmospheric Composition and

¹Now at Department of Atmospheric Science, Colorado State University, Fort Collins, Colorado, USA.

Structure: Instruments and techniques; 0345 Atmospheric Composition and Structure: Pollution—urban and regional (0305); **KEYWORDS:** PM-2.5, light scattering, aerosol optical depth, aerosol radiative forcing

Citation: Carrico, C. M., M. H. Bergin, J. Xu, K. Baumann, and H. Maring, Urban aerosol radiative properties: Measurements during the 1999 Atlanta Supersite Experiment, *J. Geophys. Res.*, 108(D7), 8422, doi:10.1029/2001JD001222, 2003.

1. Introduction

[2] The southeastern United States has experienced a substantial increase in population over the past several decades. In particular, the Atlanta metropolitan area population has grown by nearly 40% within the last 10 years. Associated with this population increase are increases in the emissions of anthropogenic pollutants from a variety of stationary and mobile sources. These pollutants include particulate matter, which is directly emitted (e.g., soot and trace metals) as well as formed in the atmosphere from the reactions of gaseous precursors (such as NO_x , SO_2 , and VOCs). For example, Atlanta is well known for its lack of compliance with O_3 standards and was frequently out of compliance during this experiment (P. V. Solomon et al., unpublished manuscript, 2001a). Also of particular concern is the fraction of aerosol mass having diameters less than $2.5 \mu\text{m}$ ($\text{PM}_{2.5}$), since these particles are believed to most adversely affect human health [Wilson and Suh, 1997; Weber et al., 2003a]. With the impending implementation of EPA National Ambient Air Quality Standards (NAAQS) for $\text{PM}_{2.5}$, a substantial portion of the eastern United States may be out of attainment [Parkhurst et al., 1999]. Thus it is important to understand the sources and processes responsible for the observed concentrations of $\text{PM}_{2.5}$ in potential nonattainment areas, such as metro Atlanta, so that appropriate control strategies can be developed.

[3] In addition to health impacts, $\text{PM}_{2.5}$ efficiently scatters and absorbs solar radiation thus impacting atmospheric visibility [Waggoner et al., 1981]. Moreover, U.S. trends in visibility show that over the last few decades the area of maximum visibility degradation has shifted in season from winter to summer and in location from the Ohio River Valley further southeast and in the region around the Great Smoky Mountains [Husar and Wilson, 1981, 1993; Malm et al., 2000]. Based on historic observations of visual range (L_v), Husar and Wilson [1993] show that since 1960 visibility has decreased by as much as 30% in many parts of the southeastern United States due to increases in $\text{PM}_{2.5}$. Additionally, by their interactions with atmospheric radiation as well as the paramount role of aerosols in cloud formation, aerosols are thought to influence climate through the perturbation of the global energy balance [Charlson et al., 1992; Penner et al., 1994; Schwartz, 1996; Intergovernmental Panel on Climate Change (IPCC), 2001]. Also, the attenuation of solar radiation by aerosols may also influence photosynthesis [Chameides et al., 1999; Cohan et al., 2002] and atmospheric photochemistry and thus modify the concentrations of species such as O_3 [Chang et al., 1987; Jacobson, 1997; Dickerson et al., 1997].

[4] The key parameter determining the influence of aerosols on visibility is the aerosol light extinction coefficient (σ_{ep}), the sum of the aerosol light scattering (σ_{sp}) and absorption coefficients (σ_{ap}). The influence of aerosols on climate, photochemistry as well as crop production depends on several additional factors. These parameters include the

aerosol optical depth ($\delta_a(\lambda)$, the integral of σ_{ep} with height), aerosol single scattering albedo (ω_0 , the ratio of σ_{sp} to σ_{ep}), and the aerosol upscatter fraction [Coakley and Chylek, 1975; Haywood and Shine, 1995; Russell et al., 1997]. Due to a lack of pertinent aerosol measurements, the above mentioned aerosol influences have yet to be systematically addressed, particularly in the southeastern United States [Yu et al., 2001].

[5] This paper discusses $\text{PM}_{2.5}$ optical properties sampled near ground level during the Atlanta Supersite study conducted from 30 July to 3 September 1999. Measurements include σ_{sp} and σ_{ap} , measured at low (RH < 50%) instrumental relative humidity, as well as $\text{PM}_{2.5}$, elemental carbon (EC) and organic carbon (OC) mass concentrations. In addition, multistage impactor measurements are used to estimate σ_{sp} and σ_{ap} as a function of D_p in order to determine the particle sizes responsible for light extinction. The above measurements also allow estimation and comparison of mass scattering and absorption efficiencies via several means. Column measurements of the aerosol optical depth at several visible wavelengths are also presented, and finally, the direct shortwave radiative forcing by aerosols is estimated based on column and surface radiative measurements.

2. Experimental Methods

[6] As part of the Atlanta Supersite 1999 experiment, measurements of $\text{PM}_{2.5}$ aerosol properties were conducted from 30 July through 3 September 1999 at the Jefferson Street Site near downtown Atlanta, GA (P. V. Solomon et al., unpublished manuscript, 2001a). As shown in the schematic in Figure 1, air was sampled at a flow rate of 16.7 L min^{-1} through a $\text{PM}_{2.5}$ cyclone (URG, Inc.) located $\sim 7 \text{ m}$ above ground level. Flow was maintained with vacuum pumps (Gast, Inc.) and controlled using critical orifices (O'Keefe Controls, Inc.) downstream of all the instrumentation. After passing through the cyclone, the aerosol flowed into a sampling shelter via 7 m of 0.95 cm ID black conductive antistatic tubing.

[7] RH control was accomplished via mild heating of a 30 cm section of 1.27 cm ID stainless steel tubing to maintain an RH < 50% with an RH controller (Watlow Instruments, Inc.). A capacitive type sensor (Vaisala Humicap 50Y) was used for RH measurement and was recently factory calibrated with a manufacturer stated uncertainty of $\pm 2.5\%$ at RH = 50%. The aerosol RH was maintained at $49 \pm 5\%$ (all values presented as such are arithmetic means \pm standard deviations) in order to minimize the influence of condensed water on measured properties [Ogren, 1995; Bergin et al., 2001]. This RH was chosen to reduce RH dependence of aerosol properties [Tang, 1996, 1997] while avoiding potential aerosol crystallization at lower RH and while minimizing sample heating. The parameter most sensitive to a change in RH among those discussed here is the mass scattering efficiency (E_{sp} , which is σ_{sp} divided by $\text{PM}_{2.5}$

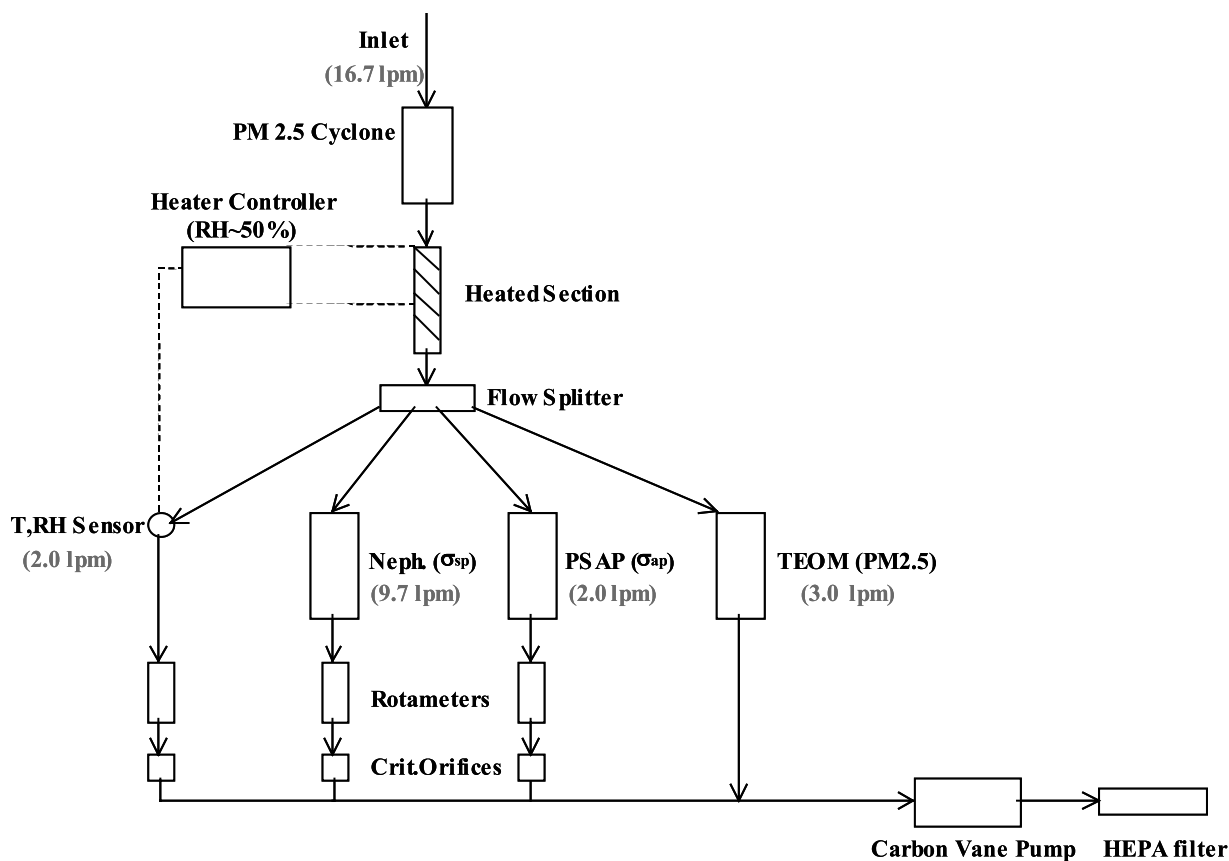


Figure 1. Flow diagram for measurement of aerosol optical and physical properties at the Atlanta Supersite 1999 study.

mass concentration), and the temporal correlation between hourly average sample RH and E_{sp} is $R^2 = 0.08$.

[8] The average ambient temperature and RH during this study in Atlanta were $26.8 \pm 4.0^\circ\text{C}$ and $63 \pm 19\%$, respectively. The average sample temperature and RH were $31.1 \pm 3.5^\circ\text{C}$ and $48 \pm 5\%$, respectively, for the nephelometer and other instruments shown in Figure 1. Thus the sample heating was $\sim 5^\circ\text{C}$, and at no time was the sample temperature heated above 39°C . Laboratory volatility studies with pure ammonium nitrate aerosol at very low RH showed modest (~ 10 – 20%) losses of submicrometer particles for temperatures up to 40°C and with residence times used here [Dougle and ten Brink, 1996; Bergin et al., 1997]. Though the sizable organic carbon content may also be subject to volatility losses as well, less than 3% of the $\text{PM}_{2.5}$ mass was nitrate in Atlanta (P. V. Solomon et al., unpublished manuscript, 2001b), and the aerosol was still likely hydrated also inhibiting volatility losses.

[9] After RH conditioning, the aerosol was split into four separate insulated pathways using a flow splitter (URG, Inc.). One line passed over a temperature/RH sensor at 2.0 L min^{-1} that was used to control the sample RH. In a second line, light scattering coefficients (σ_{sp}) were measured with an integrating nephelometer at a wavelength of 530 nm (Radiance Research Inc., M903 nephelometer). The nephelometer was calibrated several times during the field experiment using clean filtered air and HFC-134a as the calibration gases. As a result of geometrical limitations, the integrating nephelometer is subject to angular truncation

errors and other nonidealities, as it cannot detect the entire phase function of scattered light. These nonidealities have been characterized for a similar instrument [Anderson and Ogren, 1998], but as of yet not thoroughly quantified for the instrument used in this study. Nonetheless, this correction is modest for an accumulation mode aerosol, e.g., a 4% increase in σ_{sp} for a polluted aerosol with a sub $1 \mu\text{m}$ size cut using a similar instrument [Carrico et al., 2000].

[10] In a third line, the light absorption coefficient (σ_{ap}) was measured at a wavelength of 565 nm using a filter-based light transmission technique (Radiance Research Inc., Particle Soot Absorption Photometer) and was corrected for light scattering effects using the algorithm of Bond et al. [1999]. Though the σ_{ap} measurement is at an effective instrumental wavelength of 565 nm, the calibration of Bond et al. [1999] adjusts this to 550 nm.

[11] A fourth line was used to measure the $\text{PM}_{2.5}$ mass concentration with a continuous method that uses vibration frequency of mass deposited on a filter (Rupprecht and Patashnick, Inc., Tapered Element Oscillating Microbalance or TEOM) [Patashnick and Rupprecht, 1991]. In order to minimize interference from adsorption/desorption of water vapor caused from fluctuations in sample RH or moderate cycling of room temperature and RH that has been observed at lower sample temperatures, the instrument was operated with sample temperature of $T = 50^\circ\text{C}$. Several studies have examined potential volatility losses with TEOM sampling with heating to 50°C showing losses of $\sim 20\%$ are possible [Ayers et al., 1999]. However, losses affecting the measure-

ments are most pronounced during winter sampling when sample heating is greatest, when examining high time resolution data (\sim minutes), and where nitrate or wood smoke is a dominant species [Meyer *et al.*, 2002; Okrent, 1998; Allen *et al.*, 1997]. None of these are the case here, as this study examines hourly averaged data during summer at a site where nitrate is a small component (2–3%) of $PM_{2.5}$ and wood smoke is negligible [Butler *et al.*, 2003; P. V. Solomon *et al.*, unpublished manuscript, 2001b].

[12] With a TEOM sample temperature of 50°C and an average ambient dew point temperature of $18.4 \pm 3.4^\circ\text{C}$, the TEOM sample RH was $17 \pm 3\%$ during the Atlanta Supersite 1999 study. All the mass and optical measurements are at a low RH where particle diameter, though not independent of RH, is much less sensitive to RH than for $RH > 60\%$ [Tang, 1996, 1997]. As discussed below, the low influence of RH variation in this study is seen in the low correlation between sample RH and light scattering efficiency E_{sp} , agreement in mass measurements, and as seen in laboratory studies with salts commonly found in ambient aerosols [Tang, 1997].

[13] In addition, the aerosol optical depth ($\delta_a(\lambda)$) was estimated based on measurements made with a hand-held Sun photometer (Solar Light Company, Microtops II) and using a method similar to that described by Reddy *et al.* [1990]. The wavelengths for $\delta_a(\lambda)$ measurements are 380, 440, 500, 675, 870, and 1020 nm and are in windows such that absorption by ozone and water vapor do not interfere with the measurement [Thekaekara, 1973]. For each measurement the optical depth was determined using the relationship $\delta_a(\lambda) = -1/m * \ln(I_\lambda/I_{0,\lambda})$, where m is the air mass (which is defined as the secant of the solar zenith angle), I_λ , the measured surface irradiance, and $I_{0,\lambda}$ the solar constant. The solar constant was determined for each wavelength using the Langley plot method and based on calibrations obtained at Mauna Loa Observatory [Shaw, 1983]. For each measurement, the calibration values were used to estimate the specific solar constant by correcting for the Sun-to-Earth distance and by subtracting the optical depth due to the Rayleigh scattering of gas molecules [Reddy *et al.*, 1990]. The measurements of σ_{sp} , σ_{ap} , and $\delta_a(\lambda)$ are compared at the proximate wavelengths of 530, 550, and 500 nm, respectively, where the measurements are available. Though these are different wavelengths, they are all close to the peak in the solar spectrum [Thekaekara, 1973].

[14] To investigate the particle size dependence of light extinction, samples were collected for determination of aerosol mass and elemental carbon (EC) concentrations as a function of D_p using Micro-Orifice Uniform Deposit Impactors (MOUDI) [Marple *et al.*, 1991]. For parallel sampling lines, air was drawn through 10 m of 5 cm ID aluminum tubing at 120 L min^{-1} followed by a flow splitter and ~ 0.5 m of 1 cm ID stainless steel tubing preceding the MOUDIs. The MOUDI sample conditions of $T = 30.2 \pm 2.3^\circ\text{C}$ and $RH = 47 \pm 7\%$ were close to the sampling conditions for the σ_{sp} and σ_{ap} measurements ($RH = 49 \pm 5\%$) facilitating comparison with optical measurements. However, using this sample RH in the MOUDI for the uncoated substrates used in this measurements may have increased particle bounce as, for example, Stein *et al.* [1994] found $RH = 70\text{--}80\%$ optimum for minimizing particle bounce. The MOUDIs were preceded by a $2.5 \mu\text{m}$ cyclone,

and 50% cut-off diameters for the MOUDI stages are 1.78, 0.97, 0.56, 0.32, 0.18, 0.098 and $0.056 \mu\text{m}$. The sample substrates (aluminum foil on stages and quartz fiber filters as after filters) were combusted at 500°C for 4 h, allowed to cool, and then stored at room temperature in similarly cleaned glass jars. After sample collection, the foils and filters were handled in a clean hood and later conditioned at $RH = 40\%$ and $T = 20^\circ\text{C}$ for one week in a clean room. Mass size distribution samples ($n = 7$) and EC mass size distributions ($n = 56$) were collected over ~ 3 day and ~ 10 h sampling periods, respectively. Aerosol masses were determined using a microbalance (Cahn, Inc.) while EC was determined at Desert Research Institute (DRI) using a thermal evolution technique [Chow *et al.*, 1993]. The opaque aluminum foil substrates of the MOUDI do not permit an optical correction for charring of organic carbon. Thus the temperature determined as the EC/OC split point in coincident bulk quartz filter samples was used as the EC/OC split temperature for the MOUDI samples. This approach assumes that the EC/OC split temperature does not change with particle size. This assumption was made as adsorbed volatile and semivolatile organic compounds likely dominate the MOUDI after-filter whereas less volatile, higher molecular weight compounds likely dominate the carbon on bulk aerosol filters.

[15] In addition, 24 h $PM_{2.5}$ mass and carbon measurements at ambient RH were made on Teflon and quartz filters, respectively. Mass difference measurements were made with a microbalance (Mettler Toledo Inc., MT-5) after approximately two weeks equilibration time in a clean room at $T = 20^\circ\text{C}$ and $RH = 40\%$. The carbon analysis of 24-h quartz filter samples used the thermo-optical technique of Birch and Cary [1996] that incorporates an optical charring correction in the analysis technique. For the carbon filter analysis, no corrections for adsorbed gas-phase semivolatile organic carbon compounds were considered though this is presumed to be minor as the quartz filter was preceded by a XAD coated denuder using the procedure of Gundel and Lane [1999].

[16] EC and OC measurements were also made using an on-line high time resolution technique [Rupprecht *et al.*, 1995]. The Rupprecht and Patashnick Series 5400 Ambient Carbon Particulate Monitor uses a nondispersive infrared detector for measuring thermally evolved CO_2 . The measurement is performed at 50°C and thus an average RH of 18%, and during the analysis carbon is evolved in a two step heating process at temperatures of 340 and 750°C for separation into organic and soot carbon. The lower limit 50% collection efficiency of the instrument is at $D_p = 0.14 \mu\text{m}$, and the instrument was preceded by a $PM_{2.5}$ cyclone. Since the entire heating cycle is done in air, an artifact due to charring of OC is expected to be minimal.

3. Results and Discussion

3.1. Average Measured Properties of the Urban Aerosol

[17] These results demonstrate a substantial urban haze layer in Atlanta as shown in Table 1 giving a summary of averages for various aerosol properties (aerodynamic $D_p < 2.5 \mu\text{m}$) during the Supersite 1999 experiment (30 July through 3 September 1999). Annual trends in $PM_{2.5}$ phys-

Table 1. Summary of Aerosol Properties (Arithmetic Mean, Standard Deviation, and Coefficient of Variation of Hourly Averages) Measured During the Supersite 1999 Study in Atlanta, Georgia, From 30 July to 3 September 1999

	σ_{sp} , 530 nm; Mm^{-1}	σ_{ap} , 550 nm; Mm^{-1}	ω_0	δ_{a} , 500 nm	L_v , km	$\text{PM}_{2.5}^{\text{a}}$, $\mu\text{g m}^{-3}$
Mean	121	16	0.87	0.44	15	31
Standard deviation	48	12	0.08	0.22	8	12
COV	0.40	0.75	0.09	0.50	0.53	0.39

^aAs determined from R & P Tapered Element Oscillating Microbalance.

ical and chemical properties as described by *Butler et al.* [2003] show that $\text{PM}_{2.5}$ mass concentrations annually at four Atlanta sites are approximately $20 \mu\text{g/m}^3$, one third smaller than the average measured during this study. However, as found by *Butler* [2000] and *Butler et al.* [2003], the summer in Atlanta historically has the highest $\text{PM}_{2.5}$ concentrations ranging from 28 to $31 \mu\text{g m}^{-3}$ at four metro Atlanta sites, comparable to these measurements. Conversely, though winter is the period with the peak contribution from nitrate, $\text{PM}_{2.5}$ concentrations are generally the lowest and in the range of $10\text{--}15 \mu\text{g/m}^3$ [*Butler et al.*, 2003]. In general terms, the $\text{PM}_{2.5}$ properties during this sampling campaign are a reasonable characterization of summertime $\text{PM}_{2.5}$ properties in the greater Atlanta metro area [*Russell et al.*, 2000].

[18] Average light scattering and absorption coefficients by particles (σ_{sp} at 530 nm and σ_{ap} at 550 nm) during the field experiment are $121 \pm 48 \text{ Mm}^{-1}$ and $16 \pm 12 \text{ Mm}^{-1}$, respectively (all values presented as such are arithmetic means \pm standard deviations). The light extinction by particles (σ_{ep}) is an order of magnitude larger than the Rayleigh scattering contribution from air underscoring the predominance of aerosol particles to light extinction in the urban atmosphere. Although σ_{ep} of the urban aerosol is dominated by σ_{sp} , σ_{ap} also makes a substantial (13%) contribution to σ_{ep} as has been found characteristic of urban areas [*Horvath*, 1995]. The magnitude of σ_{sp} in Atlanta is comparable to measurements of dry σ_{sp} in 1980 in a polluted urban site in the southeastern United States (Houston, TX) where $\sigma_{\text{sp}} = 160 \text{ Mm}^{-1}$ and a rural site (Virginia) where $\sigma_{\text{sp}} = 120 \text{ Mm}^{-1}$ [*Waggoner et al.*, 1983]. Compared to more recent measurements, σ_{sp} in Atlanta is considerably larger than nonurban polluted sites in North America and Europe including Bondville, IL, southern Great Plains, OK, Sable Island, NS, and Sagres, Portugal where σ_{sp} (550 nm) $\sim 30\text{--}50 \text{ Mm}^{-1}$ and is much larger than background continental and marine sites including Mauna Loa, HI, Cape Grim, Australia, South Pole, and Barrow, AK where $\sigma_{\text{sp}} = 5\text{--}10 \text{ Mm}^{-1}$ (these measurements are at 550 nm and for a size cut of $D_p < 1 \mu\text{m}$ at RH < 40%) [*Ogren*, 1995; *Carrico et al.*, 1998, 2000; *Koloutsou-Vakakis et al.*, 2001; *Delene et al.*, 2001]. However, the magnitude of σ_{sp} in Atlanta is comparable to nonurban sites in the southeast United States including the IMPROVE sites of Shenandoah and Great Smokies where annual average ambient total light scattering coefficients range from $100 < \sigma_{\text{sp}} < 125 \text{ Mm}^{-1}$ [*Malm et al.*, 1994, 2000]. The IMPROVE measurements are at ambient RH and are annual averages and thus not directly comparable to these results. Nonetheless, the high values in this region suggest the presence of a

regional haze in the southeast United States. The contribution of this regional haze to the air quality in Atlanta is likely substantial in addition to the urban sources of pollution. Compared to urban and rural sites in eastern China including Beijing, China, where $\sigma_{\text{sp}} = 488 \text{ Mm}^{-1}$ and $\sigma_{\text{ap}} = 83 \text{ Mm}^{-1}$ for a size cut of $D_p < 2.5 \mu\text{m}$, the impact of aerosols on atmospheric light extinction is less in Atlanta by a factor of four [*Bergin et al.*, 2001; *Xu et al.*, 2002]. Though σ_{ep} in Atlanta is considerably less than some newly industrializing and developing regions, σ_{ep} is an order of magnitude greater than Rayleigh scattering by gases and significantly impacts atmospheric light extinction in Atlanta.

[19] Based on the measurements of σ_{sp} and σ_{ap} , an estimate of the single scattering albedo in Atlanta is $\omega_0 = 0.87 \pm 0.08$. Once again these are low RH measurements and the influence of higher RH would result in larger values of ω_0 [*Russell et al.*, 2002]. The single scattering albedo measured in Atlanta is slightly lower than those found in the TARFOX and ACE-2 studies that examined regionally polluted air masses downwind of urban-industrial regions where $0.9 < \omega_0 < 0.95$ [*Russell et al.*, 1997, 2002]. The lower Atlanta ω_0 demonstrates a greater relative importance of light absorbing species, characteristic of the urban environment and found similarly in the case of Beijing, China, where $\omega_0 = 0.81 \pm 0.08$ [*Bergin et al.*, 2001]. Historical measurements in the United States during the 1970s and 1980s show an even greater role of light absorption with $0.5 < \omega_0 < 0.6$ for industrial urban areas and $0.73 < \omega_0 < 0.87$ in residential urban areas [*Waggoner et al.*, 1981]. It is not clear whether these differences are related to measurement uncertainties in σ_{ap} or the fact that soot emissions have been substantially reduced over the last few decades.

[20] An upper limit to the visual range (L_v) is estimated using the measurements here and a modified Koschmeider relationship with $L_v = 1.9/\sigma_e$, where σ_e is the extinction due to scattering and absorption by particles and gases [*Griffing*, 1980; *Husar and Wilson*, 1993]. Assuming a negligible contribution from light absorption by gases and an additional contribution of Rayleigh scattering by gases ($\sim 13 \text{ Mm}^{-1}$ at 550 nm), using measured σ_{sp} and σ_{ap} at RH = 50% gives an upper bound of $L_v = 15 \pm 8 \text{ km}$. Given that ambient RH = $63 \pm 15\%$, L_v is likely 33–50% lower on average due to the influence of RH between 50 and 63% [*Covert et al.*, 1979; *Malm et al.*, 2000]. This reduction in visibility will be even greater during times of high RH and when there are dominant contributions from strongly hygroscopic species such as sulfuric acid [*Tang*, 1996].

[21] Mean concentration of $\text{PM}_{2.5}$ as measured by the TEOM is $31 \pm 12 \mu\text{g m}^{-3}$. Mean values for TEOM, filter and MOUDI $\text{PM}_{2.5}$ measurements at the same site fall within a narrow range of 26 to $34 \mu\text{g m}^{-3}$ (Table 2); the reader is referred to S. V. Hering et al. (unpublished manuscript, 2001), H.-J. Lim et al. (unpublished manuscript, 2001), *Weber et al.* [2003b], and P. V. Solomon et al. (unpublished manuscript, 2001b) for more detailed inter-comparisons of mass and chemistry measurements. TEOM measurements at several other metro Atlanta locations are within 10% demonstrating the spatial homogeneity of average $\text{PM}_{2.5}$ within Atlanta [*Butler*, 2000, *Butler et al.*, 2003]. Although this study covered only approximately a one-month sampling period, our measured $\text{PM}_{2.5}$ is roughly a factor of two larger than the EPA proposed annual average

Table 2. Comparison of OC, EC and PM_{2.5} Mass Measurements and Resulting Mass Scattering and Absorption Efficiencies From Several Methods^a

	OC, μg m ⁻³	EC, μg m ⁻³	PM _{2.5} , μg m ⁻³	E _{ap} , m ² g ⁻¹	E _{sp} , m ² g ⁻¹
TEOM	–	–	31 ± 12	–	3.8 ± 0.7
Filter	7.7 ± 2.5	0.8 ± 0.4	34 ± 10	18.3 ± 5.9	3.5 ± 0.5
MOUDI	7.9 ± 2.0	1.7 ± 0.9	26 ± 5	9.5 ± 1.5 ^b	4.4 ± 0.2
R & P 5400	7.9 ± 2.6	2.8 ± 1.6	–	5.3 ± 1.8	–

^aMOUDI results represent sum of all impactor stages including the quartz after-filter (37%, 13%, and 1% of the OC, EC, and PM_{2.5} masses, respectively).

^bBased on Measured EC mass size distribution and Mie calculated light absorption. Using MOUDI measured mass and measured light absorption gives $9.3 \pm 3.2 \text{ m}^2 \text{ g}^{-1}$.

standard of $15 \mu\text{g m}^{-3}$. However, the daily average PM_{2.5} ranges from 11 to $44 \mu\text{g m}^{-3}$, well below the 24-h average proposed standard of $65 \mu\text{g m}^{-3}$. Though these results are only a small snapshot in time, they suggest Atlanta's PM_{2.5} compliance problem is related to persistent rather than episodic causes. Aerosol carbon was measured using several techniques during the experiment (P. V. Solomon et al., unpublished manuscript, 2001b; H.-J. Lim et al., unpublished manuscript, 2001). Average elemental carbon (EC) results from several techniques are also given in Table 2, and will be discussed further below.

3.2. Aerosol Variability in the Context of Meteorology and Aerosol Sources

[22] Despite the relatively dry, stagnant synoptic conditions particularly during the first three weeks of the experiment (J. C. St. John et al., unpublished manuscript, 2001), aerosol properties measured during Atlanta Supersite 1999 demonstrate large variability over timescales ranging from minutes to days (the Atlanta Supersite 1999 study; Figure 2). The coefficient of variation (COV), the standard deviation divided by the mean value, can be used to compare the variability of different data sets. As shown in Table 1 and Table 2, extensive aerosol parameters (those depending on aerosol concentration such as PM_{2.5}, σ_{sp} , and σ_{ap} with $0.4 < \text{COV} < 0.8$) showed much greater variability than intensive aerosol properties (those independent of aerosol concentration such as ω_0 with $0.1 < \text{COV} < 0.3$). The lower variability in aerosol intensive properties suggests that their controlling influences such as aerosol size distribution, relative chemical composition, and particle morphology had variability less important to aerosol radiative properties than changes in PM_{2.5} mass concentration.

[23] In general, synoptic conditions during the first three weeks of the field intensive favored the formation and retention of pollutants in the atmosphere including weak pressure gradients, high pressure and high temperature (J. C. St. John et al., unpublished manuscript, 2001). The field intensive had three precipitation events indicated in the Atlanta Supersite 1999 study (Figure 2) each showing pronounced effects on aerosol properties (Table 3), most dramatically and rapidly on PM_{2.5} and σ_{sp} . Precipitation scavenging of aerosols is one of the most important atmospheric cleansing mechanisms [Dickerson et al., 1987] and has been found to dramatically affect aerosol optical properties in other studies [Bergin et al., 2001]. Precipitation

effects can be investigated for the Radiance Research light scattering and absorption and the Rupprecht and Pataschnick mass and carbon measurements as a result of their high time resolution in contrast to the time-integrated sampling methods.

[24] The first two short precipitation events (8 August, 1400–1900 local time (LT) and 20 August, 1500–1600 LT) had accumulations of 12 and 3 mm, respectively, though they resulted in substantial decreases in PM_{2.5} and σ_{sp} (~50%) over several hours (Figure 2, Table 3). The third precipitation event (from 1400 on 23 August to 1900 on 25 August) occurred over two days (42.1 mm) and is the result of the passage of a frontal system through Georgia (J. C. St. John et al., unpublished manuscript, 2001). The result was a dramatic drop in PM_{2.5} concentration and σ_{sp} by a factor of ~3 (Table 3). The heaviest rain (34.8 mm) occurred during the period from 0730 to 0930 on 24 August and corresponds to a decrease in σ_{sp} from ~150 to 20 Mm^{-1} . Also, ambient RH was frequently above 90% beginning ~0000 LT on 24 August and lasting until ~0800 LT on 26 August, indicating the likelihood of fog formation and coinciding with the trough in PM_{2.5} and σ_{sp} . The scavenging of particles by fog and precipitation droplets is the likely predominant removal mechanism responsible for the decrease in PM_{2.5} and σ_{sp} during this period. A lingering synoptic-scale influence on aerosol optical properties associated with the frontal passage is evident in Figure 2, as the PM_{2.5} and σ_{sp} remain low until 27 August after the precipitation and fog events.

[25] Despite the strong influence of precipitation and fog events on PM_{2.5} and σ_{sp} , the concentration of OC, EC, and σ_{ap} show smaller decreases (Figure 2, Table 3). This is particularly the case for σ_{ap} , though the third prolonged rain event causes a decrease in σ_{ap} as well (Figure 2, Table 3). The changes in σ_{ap} and σ_{sp} also affect ω_0 , particularly during the precipitation event on 23–25 August where ω_0 decreases from 0.95 to 0.4 over the course of 9 h (Figure 2). The contrasting changes in aerosol properties during the precipitation events demonstrate some degree of external mixing of more water-soluble light scattering and the less water-soluble light absorbing compounds.

[26] As discussed in more detail below, the geometric mean light scattering and absorption D_p are $0.54 \mu\text{m}$ and $0.13 \mu\text{m}$, respectively, both in the range of minimum precipitation scavenging efficiency. Typically, precipitation scavenging has a minimum efficiency in the range $0.1 \mu\text{m} < D_p < 1 \mu\text{m}$ where neither diffusion nor interception/impaction are efficient removal mechanisms [Dickerson et al., 1987]. Elemental carbon, the light-absorbing component of the soot aerosol, is typically hydrophobic due to the nonpolar nature of the carbon-carbon bonds [Andrews and Larson, 1993]. The hydrophobic nature of EC may strongly suppress the activation of these particles and their incorporation into cloud/fog droplets, diminish precipitation scavenging, and increase its residence time during these events. The results here suggest that aerosol solubility is strongly linked to the aerosol atmospheric lifetime as has been suggested in previous studies showing EC enrichment of the interstitial aerosol found in fog events [Noone et al., 1992].

[27] A clear diel pattern is apparent in the hourly averaged intensive and extensive aerosol properties as shown in

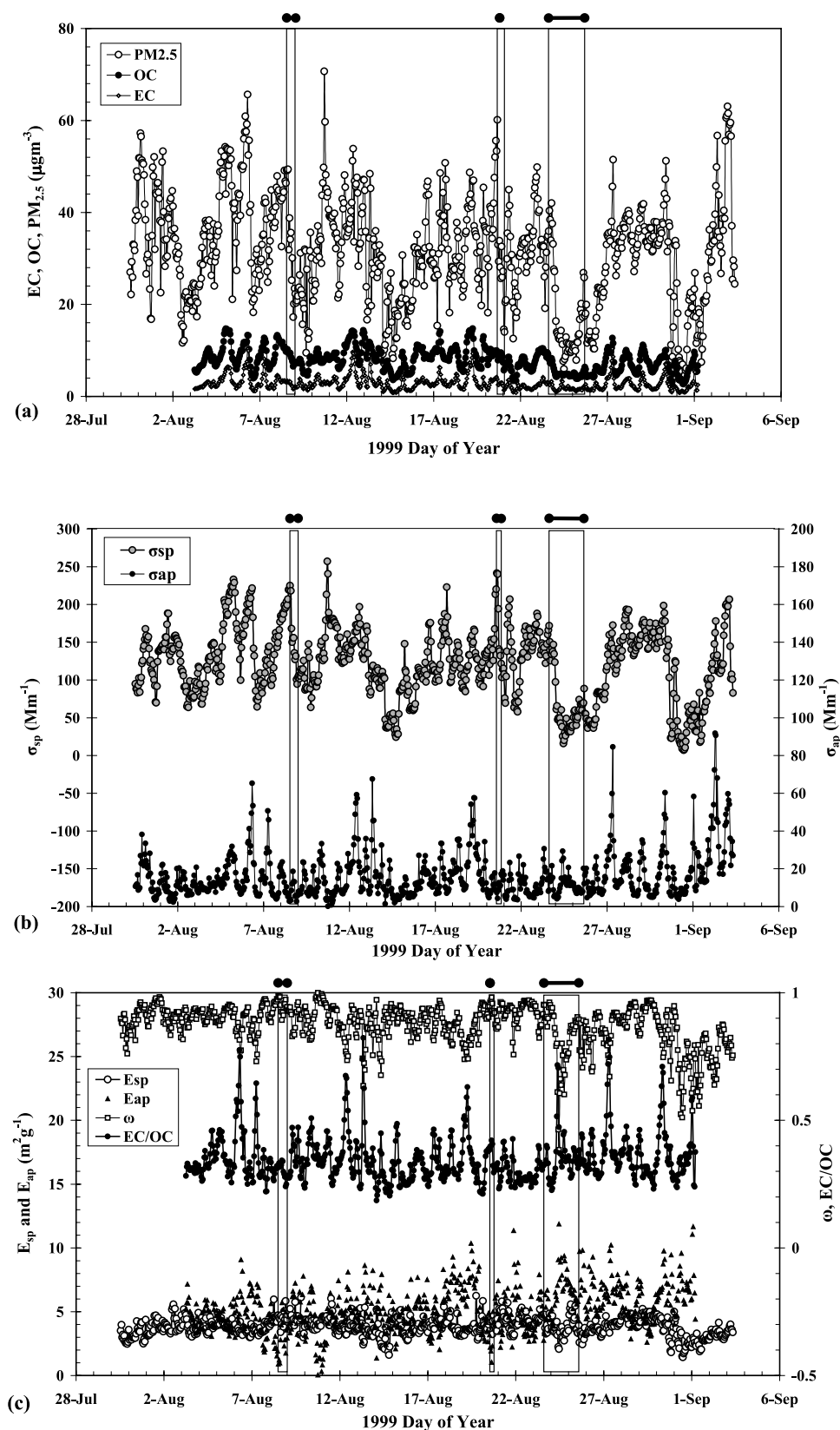


Figure 2. Time series of (a) EC, OC (R & P Series 5400 Ambient Particulate Carbon Monitor) and $PM_{2.5}$ mass concentrations (R & P TEOM) (b) aerosol midvisible total light scattering (Radiance Research nephelometer) and absorption (Radiance Research PSAP) coefficients (σ_{sp} and σ_{ap}) for particles with $D_p < 2.5 \mu m$ and controlled RH = $49 \pm 5\%$, and (c) aerosol mass scattering and absorption efficiencies (E_{sp} and E_{ap}), single scattering albedo (ω_0), and EC/OC ratio. Three precipitation periods are indicated.

Table 3. Comparison of Five Hour Average Aerosol Properties Before and After Three Precipitation Events During the Atlanta Supersite 1999 Study on 8, 20, and 23–25 August 1999

	σ_{sp} , 530 nm; Mm^{-1}	σ_{ap} , 550 nm; Mm^{-1}	ω_0	$PM_{2.5}^a$, $\mu g\ m^{-3}$	$OC_{2.5}^a$, $\mu g\ m^{-3}$	$EC_{2.5}^a$, $\mu g\ m^{-3}$
Before rain event 1	218 ± 7	4.3 ± 1.4	0.98 ± 0.01	48.1 ± 1.4	10.2 ± 0.4	3.3 ± 0.1
After rain event 1	111 ± 17	5.3 ± 1.4	0.96 ± 0.01	23.2 ± 4.9	7.4 ± 0.7	2.0 ± 0.3
Before rain event 2	216 ± 30	10.0 ± 5.1	0.95 ± 0.03	50.1 ± 5.4	9.7 ± 0.2	3.9 ± 0.2
After rain event 2	127 ± 15	13.7 ± 3.1	0.90 ± 0.01	30.0 ± 3.4	8.9 ± 0.7	2.7 ± 0.2
Before rain event 3	146 ± 19	14.8 ± 4.3	0.91 ± 0.03	37.6 ± 4.8	9.2 ± 0.4	2.9 ± 0.2
After rain event 3	42 ± 4	8.2 ± 3.3	0.84 ± 0.06	10.9 ± 1.1	4.4 ± 0.1	1.4 ± 0.1

Figure 3 giving hourly arithmetic mean values with error bars representing one standard error. Such trends are linked to both the diel emission trends and meteorological factors such as mixing height. Aerosol extensive properties

including $PM_{2.5}$, σ_{sp} , σ_{ap} , elemental carbon concentration (EC), and organic carbon concentration (OC) peak in the morning around 0800 LT. Often times the early morning features a low altitude temperature inversion that serves as

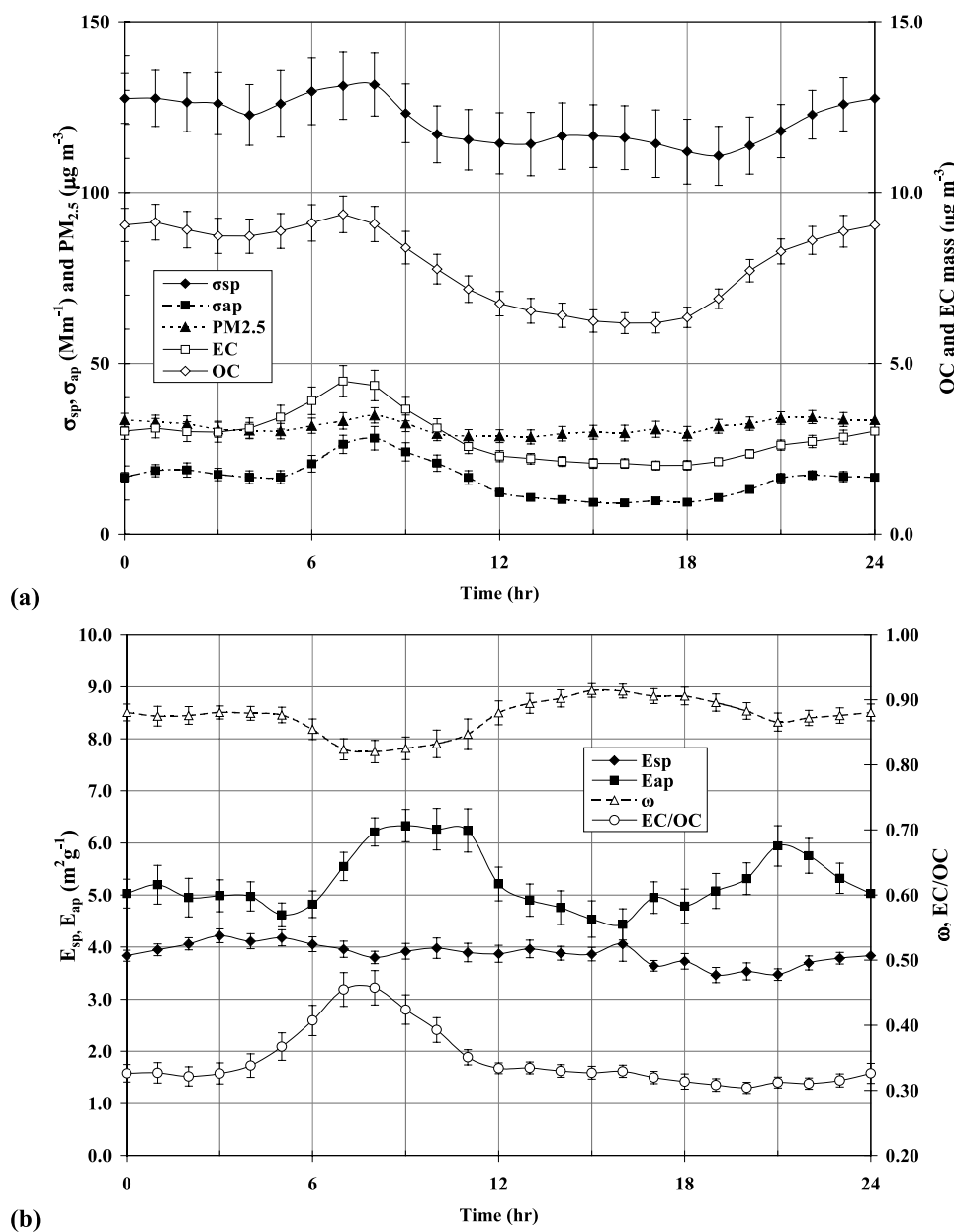


Figure 3. Diel variability of (a) extensive and (b) intensive aerosol properties in Atlanta during the Supersite 1999 study shown as hourly mean values. Error bars are the standard errors for the measurements.

a barrier to vertical mixing allowing buildup of $PM_{2.5}$ concentrations.

[28] The evidence here suggests the important influence of combustion sources associated with morning rush hour traffic. The morning peak in aerosol concentrations coincides with the peak in morning rush hour traffic in Atlanta [Ross *et al.*, 1998] and also the time period of lowest wind speeds (J. C. St. John *et al.*, unpublished manuscript, 2001) and limited vertical convective activity due to the absence of solar heating. The influence of nearby sources including local industries and a bus depot may have contributed to these trends, though the proximity to the center of the city and the dense mobile source strength in the area is also to some extent responsible [Edgerton *et al.*, 2000]. EC/OC analysis of filter samples shows that the Jefferson Street Site has an average EC/OC = 0.11 ± 0.05 from 19 filter samples between 6 and 24 h. A comparison of four Atlanta sites over a one year time period showed the Jefferson Street site to have the most pronounced diel pattern particularly in regard to the peak in EC [Butler *et al.*, 2003]. Furthermore, the measured EC/OC ratios fall into two regimes suggesting delineation between primary and secondary aerosols. In general, the periods with both high EC and OC also have elevated EC/OC ratio. These are most frequent in the morning, and thus are likely dominated by primary emissions.

[29] The morning peak at around 0800 LT is particularly pronounced for soot-related measurements including both EC and σ_{ap} that show substantial increases, from 3 to $4.5 \mu\text{g m}^{-3}$ and from 17 to 28 Mm^{-1} , respectively (Figure 3). Moreover, the EC/OC ratio as measured by the real-time R & P instrument shows a distinct peak in the morning, increasing from 0.32 to a maximum of 0.46 at 0800 LT. Fresh combustion aerosols from mobile sources and particularly diesel engines typically have a large soot component that is largely EC, and the fraction of EC in the aerosol has been related to aerosol age in other studies [Turpin and Huntzicker, 1991]. Despite the differences in trends, throughout the experiment EC and OC show a stronger correlation ($R^2 = 0.7$) than EC and $PM_{2.5}$ ($R^2 = 0.4$) suggesting similar sources categories for the carbonaceous components and likely a substantial vehicular contribution to OC as well.

[30] Aerosol radiative properties also demonstrate a diel pattern as seen in a decrease in ω_0 from 0.88 overnight to 0.82 from 0700 to 0800 LT and recovery back to 0.90 by 1200 LT. The late afternoon minimum in $PM_{2.5}$ and σ_{sp} appears characteristic of other studies. However, the morning peak is much less prevalent [Mézáros *et al.*, 1998; Carrico *et al.*, 2000] in the diel variability at nonurban polluted sites highlighting the importance of mobile sources on urban air quality.

[31] As shown in Figure 3, the morning peak in σ_{ap} is related both to an increase in EC concentration as well as an increase in the mass absorption efficiency (E_{ap} , σ_{ap} per unit mass concentration of EC) of the particles. The fresh combustion aerosol thus features both a larger EC component as well as size distribution and chemical composition that more efficiently absorbs visible radiation. This is in contrast to the diel trend of σ_{sp} which is most related to changes in $PM_{2.5}$ concentration as discussed below. Although the evening minimum in σ_{sp} is in part caused by a small ($\sim 10\%$) decrease in aerosol mass scattering efficiency (E_{sp} , σ_{sp} per unit mass concentration of $PM_{2.5}$), in

general, E_{sp} is fairly constant (no significant difference at the 95% confidence level). Furthermore, E_{sp} does not show a clear diel trend for the urban aerosol.

[32] The influence of mobile combustion sources is also apparent in the comparison of weekday to weekend aerosol properties reflecting a trend consistent with the diel variations. Though less statistically significant than the diel pattern, comparison shows a consistent trend for σ_{ap} , E_{ap} , and ω_0 during the weekdays ($14 \pm 4 \text{ Mm}^{-1}$, $5.6 \pm 1.3 \text{ m}^2 \text{ g}^{-1}$, and 0.86 ± 0.07 , respectively) compared with the weekends ($11 \pm 3 \text{ Mm}^{-1}$ and $4.6 \pm 0.7 \text{ m}^2 \text{ g}^{-1}$, and 0.92 ± 0.02 , respectively). These trends suggest the importance of vehicular sources and combustion-derived soot carbon to the Atlanta $PM_{2.5}$ problem.

[33] Beginning in the morning around 1000 LT, $PM_{2.5}$, σ_{sp} , and σ_{ap} all begin to drop. This decrease in $PM_{2.5}$ coincides with enhanced convective mixing [Seinfeld and Pandis, 1998] due to the strongly sunny and clear conditions during the experiment and as indicated by the increased wind speeds (J. C. St. John *et al.*, unpublished manuscript, 2001). Also, a drop-off in the mobile source strength with rush hour ending contributes to this trend as is particularly obvious with diel trend with EC and σ_{ap} [Ross *et al.*, 1998]. The expected evening rush hour peak demonstrates similar trends, but is much less pronounced during the evening rush hour from 1600 to 1900 LT (Figure 3). Additionally, and somewhat surprisingly, the peak is somewhat later than expected as σ_{ap} and EC reach a maximum around 2100 LT and σ_{sp} and $PM_{2.5}$ reach their local maximum at approximately midnight. This is likely due to strong afternoon convective activity and the decreasing intensity of mixing into the evening.

3.3. Aerosol Mass Scattering and Absorption Efficiencies

[34] Temporal and diel trends for the aerosol mass scattering and absorption efficiencies (E_{sp} and E_{ap} , respectively) based on real time measurements with the R & P TEOM and R & P 5400 were discussed above. Average E_{sp} and E_{ap} are now estimated based on several measurement techniques including filter samples, MOUDI sampling, TEOM, and the R & P 5400 measurements (Table 2). A relatively strong relationship is observed between TEOM measured $PM_{2.5}$ concentration and σ_{sp} ($R^2 = 0.80$, $n = 836$, sample time $t = 1$ hour) and yields $E_{sp} = 3.8 \pm 0.7 \text{ m}^2 \text{ g}^{-1}$ (Figure 4). In comparison, summing the stages of the MOUDI during the experiment for mass and calculating σ_{sp} based on mass size distributions (discussed in more detail below) yields in $E_{sp} = 4.4 \pm 0.2 \text{ m}^2 \text{ g}^{-1}$ ($R^2 = 0.96$, $n = 7$, $t = 80$ h). Examining $PM_{2.5}$ filter measurements in comparison to measured σ_{sp} gives $E_{sp} = 3.5 \pm 0.5 \text{ m}^2 \text{ g}^{-1}$ ($R^2 = 0.94$, $n = 15$, $t = 24$ h). Examining the intermediate value $E_{sp} = 3.8 \text{ m}^2 \text{ g}^{-1}$ from TEOM measurements, measurements of σ_{sp} at low RH estimate $PM_{2.5}$ with a standard deviation $\pm 22\%$ of measured $PM_{2.5}$. Thus based on these results, measurement of low RH σ_{sp} for the urban aerosol in Atlanta can be used to estimate the dry $PM_{2.5}$ concentration (and vice versa) within $\pm 22\%$ during summertime.

[35] Similar estimates of E_{sp} have been found in other studies of polluted aerosols in both urban and nonurban locations and found values from 3.5 to $4.4 \text{ m}^2 \text{ g}^{-1}$ [Dzubay *et al.*, 1982; Waggoner *et al.*, 1983; Koloutsou-Vakakis *et*

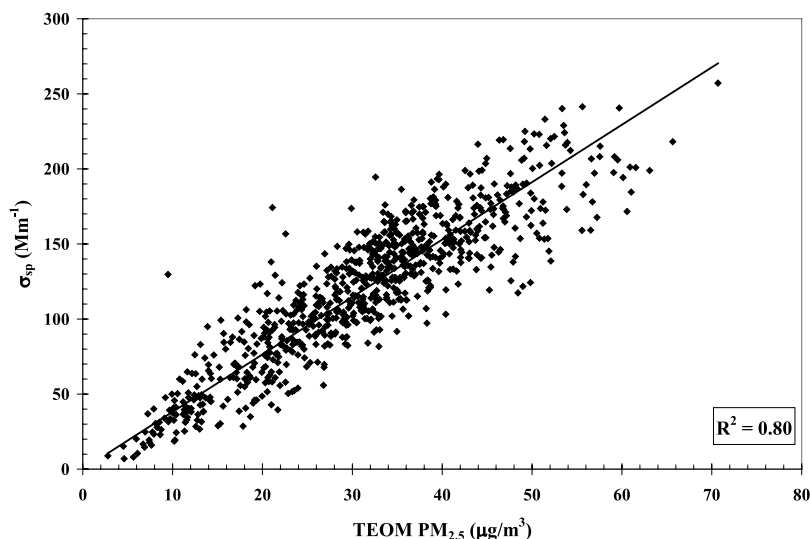


Figure 4. TEOM measured $\text{PM}_{2.5}$ mass concentrations versus aerosol midvisible total light scattering coefficient (σ_{sp}) for particles with $D_p < 2.5 \mu\text{m}$.

al., 2001]. The larger values associated with a size cut of $D_p < 1 \mu\text{m}$ (i.e., excluding the particles with $1 \mu\text{m} < D_p < 2.5 \mu\text{m}$ results in roughly the same σ_{sp} but somewhat lower $\text{PM}_{2.5}$ mass). The similarities in E_{sp} for polluted aerosols at low RH regardless of time or place is useful for modeling purposes and remarkable given the differences possible in aerosol size distribution and chemistry.

[36] A strong relationship between measured σ_{ap} and measured EC concentration (R & P 5400) is shown in μm (Figure 5; $R^2 = 0.73$) and is much stronger than the relationship between σ_{ap} and overall $\text{PM}_{2.5}$ concentration ($R^2 = 0.19$) or between σ_{ap} and OC ($R^2 = 0.37$). The mineral dust content of the aerosol was found to be small between 1 and $3 \mu\text{g}/\text{m}^3$ (P. V. Solomon et al., unpublished manuscript, 2001b). With an imaginary part of the refractive index of -0.006 for mineral dust (two orders of magnitude smaller than EC) [Teegen et al., 1996], the contribution of mineral dust to σ_{ap} is very small.

[37] However, different methods for determining EC give vastly different results for the absorption efficiency (E_{ap}) of EC. The following are arithmetic means and standard deviations of the E_{ap} calculated by taking σ_{ap} divided by EC mass concentration for each data point. As measured with the R & P 5400 in conjunction with the PSAP, a mass absorption efficiency for EC in Atlanta is $E_{\text{ap}} = 5.3 \pm 1.8 \text{ m}^2 \text{ g}^{-1}$ ($R^2 = 0.73$, $n = 696$, $t = 1$ hour). When considering only $\text{EC} < 4 \mu\text{g}/\text{m}^3$, the relationship is weaker ($R^2 = 0.41$) though $E_{\text{ap}} = 5.2 \pm 1.8 \text{ m}^2/\text{g}$, very close to the value for the entire data set. In comparison, the MOUDI measured EC size distribution and MOUDI calculated light absorption (as discussed in more detail below) gives an $E_{\text{ap}} = 9.5 \pm 1.5 \text{ m}^2 \text{ g}^{-1}$ ($R^2 = 0.97$, $n = 56$, $t = 8$ h). Likewise, in comparison to PSAP measurements, the MOUDI measured EC mass gives $E_{\text{ap}} = 9.3 \pm 3.2 \text{ m}^2 \text{ g}^{-1}$ ($R^2 = 0.79$, $n = 56$, $t = 8$ h). Filter measurements of EC using the technique of Birch and Cary [1996] in conjunction with PSAP measurements give $E_{\text{ap}} = 18.3 \pm 5.9 \text{ m}^2 \text{ g}^{-1}$ ($R^2 = 0.34$, $n = 17$, $t = 24$ h). The broad range of values for E_{ap} found in this study is summarized in Table 2 and is critically dependent on the EC measurement technique. Furthermore, calculated values

for E_{ap} show more scatter and less systematic changes than E_{sp} (Figure 2), and the average values from different methods are well outside plus or minus one standard deviation for each method (Table 2).

[38] Absorption of radiation by EC is generally ascribed an $E_{\text{ap}} \sim 10 \text{ m}^2 \text{ g}^{-1}$ at $\lambda = 515 \text{ nm}$ [Clarke, 1989; Chow et al., 1993]. However, in a review of models and measurements this value is attributed an uncertainty of at least 20% by Penner [1995]. From past studies employing a variety of techniques, a broad range of mass absorption efficiencies has been found for EC ranging from 5 to $20 \text{ m}^2/\text{g}$ [Groblicki et al., 1981; Lioussse et al., 1993]. Moreover, this range may be related to variability in aerosol properties. E_{ap} for EC has been related to the aerosol age and mixing with a range from 5 (remote) to $20 \text{ m}^2 \text{ g}^{-1}$ [Lioussse et al., 1993]. A similarly wide range of values (8 to $20 \text{ m}^2/\text{g}$) has been found in a single study during INDOEX using a single pair of techniques (black carbon from thermal evolution in conjunction with a particle soot absorption photometer) [Clarke et al., 2002]. Nonetheless, a recent side-by-side comparison of 16 carbon techniques, though demonstrating reasonable agreement for total carbon, showed a wide range of values for EC and underscored the importance of a “charring correction” for the pyrolysis of OC to EC [Schmid et al., 2001; Chow et al., 2001]. This may be related to the low E_{ap} found using the semicontinuous R & P method due to an overestimate of EC mass. Some fraction of OC may not evolve until the high temperature step or may char in the low temperature step, though likelihood of charring is lower with this method than others since the entire procedure is done in an oxygen environment.

[39] Comparing the carbon analysis techniques, similar values for OC mass were found when ignoring potential artifacts due to adsorption of gas phase species or particle bounce (Table 2). Furthermore, a strong correlation ($R^2 = 0.85$) was observed here between the high time resolution techniques (MOUDI and R & P 5400). The measurements of carbon by the MOUDI, however, included a 37% contribution to the OC and 13% contribution to the EC from the quartz after-filter (particles with $D < 0.05 \mu\text{m}$).

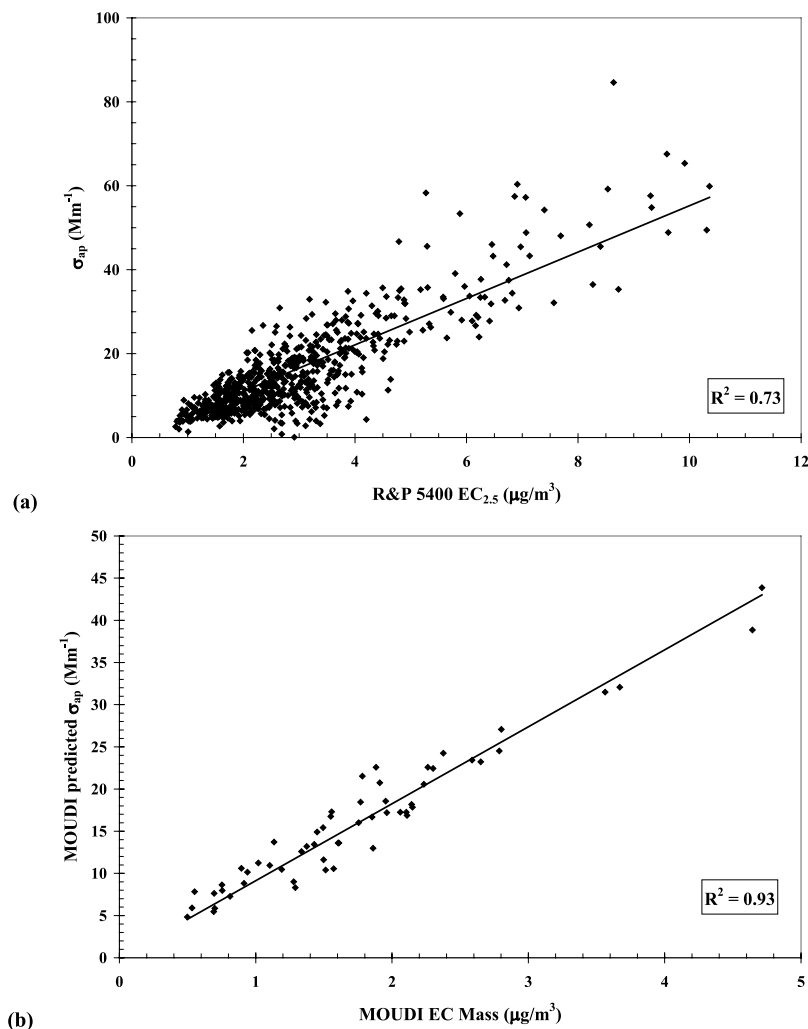


Figure 5. Light absorption efficiency as calculated from linear regressions of σ_{sp} versus EC mass concentrations for (a) R & P 5400 measured EC versus PSAP measured σ_{ap} (b) MOUDI measured EC versus MOUDI predicted σ_{ap} .

These large fractions on the after-filter are similar to past studies such as *McMurry and Zhang* [1989] who found 40–70% and 17% of the OC and EC masses, respectively, on the after-filter. The artifact here likely includes contributions from particle bounce [*Stein et al.*, 1994] and adsorption of gas phase semivolatile organics [*Turpin et al.*, 2000]. We believe adsorption of gas phase organics is the dominant process as EC and SO_4^{2-} determined in a parallel MOUDI sampler (P. V. Solomon et al., unpublished manuscript, 2001b) had nearly identical size distributions though different from that of OC. Since the EC, SO_4^{2-} , and mass size distributions showed little evidence of particle bounce, we believe the relatively elevated amounts of OC on the after-filter is most likely due to adsorption of volatile and semivolatile organic compounds. For further information, the reader is referred to a detailed intercomparison of several semicontinuous carbon (total carbon, OC, and EC) measurement techniques during the Atlanta Supersite experiment (H.-J. Lim et al., unpublished manuscript, 2001).

[40] The study of H.-J. Lim et al. (unpublished manuscript, 2001) found high correlations among carbon techni-

ques though much larger variation among techniques in the magnitude of mass concentrations for the EC mass than for OC. Though certainly variation in aerosol properties and uncertainties in the measurement of σ_{ap} contributed to the large discrepancies and variability in E_{ap} , the evidence in this study suggests a strong influence of the EC technique. Thus, although σ_{ap} and EC mass concentration are clearly linked, there still appears to be uncertainties in this interrelationship related to both measurement of light absorption and particularly the method of EC determination. A comprehensive intercomparison of light absorption including such other methods as the photo-acoustic and integrating sphere techniques in conjunction with EC measurements similar to the carbon intercomparisons of *Schmid et al.* [2001], *Chow et al.* [2001], and H.-J. Lim et al. (unpublished manuscript, 2001) would further this aim.

3.4. Aerosol Optical Properties as a Function of Particle Size

[41] To examine the size range of particles responsible for light extinction, MOUDI measurements of mass and EC are used to estimate the size dependence of σ_{sp} and σ_{ap} using

Mie theory [Bohren and Huffman, 1983]. These calculations require several assumptions including values for the aerosol particle density and the aerosol refractive index. Furthermore, the assumed density is used to convert the aerodynamic diameters measured with the MOUDI to Stokes diameters for calculation of the optical effects [Bergin *et al.*, 2001]. For the calculation of σ_{sp} , a $PM_{2.5}$ density of 1.5 g cm^{-3} and a complex index of refraction of $1.56 - 0.02i$ are assumed. The refractive index is an average value for a slightly absorbing urban aerosol [Hinds, 1999] and the real part is intermediate to those for the dominate components of the Atlanta aerosol, namely sulfate compounds (1.43 to 1.52) and carbon (1.96) with a presumed similar mass contribution from liquid water (1.33) [Seinfeld and Pandis, 1998]. The use of a bulk aerosol density of 1.5 g cm^{-3} is based on the values found for the dominant particle class by McMurry *et al.* [2002] and the values for pure ammonium sulfate and sulfuric acid of 1.8 g cm^{-3} though reduced to account for the water associated with the aerosol in these measurements at $RH \sim 50\%$.

[42] The calculation of σ_{ap} used measured EC size distributions, an EC density of 0.75 g cm^{-3} , and an EC refractive index of $1.5 - 1.0i$ as used by Horvath [1993]. The density, ρ , of soot particles has been found to vary widely given as a range of 0.75 to 1.5 g cm^{-3} [Horvath, 1993]. An assumed particle density $\rho = 0.75 \text{ g cm}^{-3}$ is used here corresponding to more numerous, smaller particles. Empirical evidence from particle density measurements (for particles in the range $0.1 < D_p < 0.3 \text{ }\mu\text{m}$ at $RH = 5$ to 10%) indicates the presence of “fluffy” soot particles with densities from $0.25 < \rho < 0.64 \text{ g cm}^{-3}$ in addition to the most abundant population of particles having $1.6 < \rho < 1.8 \text{ g cm}^{-3}$ [McMurry *et al.*, 2002]. Undoubtedly, these assumptions of particle chemistry are limiting factors in the validity of this modeling approach. Based on these assumptions and measured aerosol mass and EC size distributions, average measured and modeled σ_{sp} and σ_{ap} are shown in Table 4.

[43] For the given assumptions, the distributions of σ_{sp} and σ_{ap} at $RH \sim 50\%$ as a function of particle D_p are given in Figure 6. Also shown are the mass size distributions of $PM_{2.5}$ and EC, respectively. Geometric means ($D_{p,g}$) and geometric standard deviations for the $PM_{2.5}$ mass, EC mass, σ_{sp} , and σ_{ap} are also indicated in Figure 6. The importance of the numerous small ($D_p \sim 0.1 \text{ }\mu\text{m}$) soot particles is apparent for both the EC mass and σ_{ap} size distributions where $D_{p,g}$ (EC) = $0.27 \text{ }\mu\text{m}$ and $D_{p,g}$ (σ_{ap}) = $0.13 \text{ }\mu\text{m}$, respectively (Figure 6). The large fraction of EC mass and resulting light absorption in the first size bin ($D_p < 0.056 \text{ }\mu\text{m}$) is likely due to the influence of primary soot particles from combustion with a typical mode in the range $10 \text{ nm} < D_p < 100 \text{ nm}$ [Horvath, 1995]. The corresponding $D_{p,g}$ for mass and light scattering are $D_{p,g}$ ($PM_{2.5}$) = $0.47 \text{ }\mu\text{m}$ and $D_{p,g}$ (σ_{sp}) = $0.54 \text{ }\mu\text{m}$, respectively. Also, combining the light scattering and absorption size distributions into a light extinction distribution gives $D_{p,g}$ (σ_{ep}) = $0.45 \text{ }\mu\text{m}$ with a geometric standard deviation of 2.0.

[44] The importance of the submicrometer mode of particles to light extinction, and in particular, those having D_p near the peak of the solar spectrum of $\sim 0.5 \text{ }\mu\text{m}$ is apparent [Thekaekara, 1973]. Figure 6 shows the dominance of the accumulation mode ($0.1 < D_p < 1 \text{ }\mu\text{m}$) in contributing to both $PM_{2.5}$ mass and light scattering with a particularly

Table 4. Comparison of Measured and Modeled σ_{sp} and σ_{ap} As Averaged Over Periods of Size Distribution Measurements^a

	Number of Size Distributions	Measured Value	Modeled Value	Ratio Model/Measure
σ_{sp} , Mm^{-1}	7	119 ± 15	115 ± 24	0.95 ± 0.10
σ_{ap} , Mm^{-1}	56	15 ± 7	16 ± 8	1.12 ± 0.36

^aModel calculations use MOUDI measured mass and EC size distributions as input to a modified Mie light scattering code [Bohren and Huffman, 1983] with the assumptions detailed in the text. Measurements are averaged over the same time periods as MOUDI sampling periods and thus are slightly different than grand averages in Table 1.

narrow light scattering distribution (geometric standard deviation $\sigma_g = 1.5$). It is also worthwhile to note from Figure 6 that particle size cuts of $D_p < 1 \text{ }\mu\text{m}$ (often used in studies in radiative properties) and $D_p < 2.5 \text{ }\mu\text{m}$ (often used in health-related studies) show less than a 5% difference in σ_{ep} for the urban aerosol in Atlanta.

3.5. Aerosol Vertical Column Properties

[45] Measurements of σ_{sp} and σ_{ap} are point measurements made at the surface and at $RH \sim 50\%$. The aerosol optical depth ($\delta_a(\lambda)$) is a column-integrated measurement of light extinction (sum of scattering and absorption by aerosol particles) and inherently incorporates the influence of ambient RH and the vertical variability in σ_{ep} . Average $\delta_a(500 \text{ nm}) = 0.44 \pm 0.22$ ($n = 57$) during the Atlanta Supersite 1999 experiment and is observed to be a strong function of the wavelength of light (Figure 7). The high surface σ_{ep} demonstrates the source strength in the urban area while the correspondingly high $\delta_a(\lambda)$ indicates that elevated $PM_{2.5}$ concentrations extend beyond the surface layer throughout the boundary layer resulting in enhanced radiative effects.

[46] Assuming an exponential relationship between $\delta_a(\lambda)$ and λ , the Ångström parameters α and β are the exponential power of the best fit relationship and the value of $\delta_a(1 \text{ }\mu\text{m})$, respectively [Ångström, 1964]. Based on the 57 measured spectra of $\delta_a(\lambda)$, the best fit values for these parameters over the wavelength range of $380 \text{ nm} < \lambda < 1020 \text{ nm}$ are $\alpha = 1.5 \pm 0.3$ and $\beta = 0.15 \pm 0.07$, and with an average curve fit of $R^2 = 0.97 \pm 0.06$. Calculating α based on discrete wavelength pairs and curve fits to the average $\delta_a(\lambda)$ (Figure 7) give values within 10%. High R^2 shows the validity of the exponential relationship between $\delta_a(\lambda)$ and λ in the visible range in the case of the urban Atlanta aerosol. The relatively high value of α also underscores the predominance of submicrometer particles (i.e., whose Mie light scattering efficiency is a strong function of λ) in controlling atmospheric light extinction [Bohren and Huffman, 1983]. Correlations between α and β and between α and $\delta_a(500\text{nm})$ are quite low ($R^2 = 0.09$ and 0.01 , respectively) and suggest that drastic shifts in aerosol size distribution are not associated with periods of high optical depth. This assertion applies only to clear sky periods when Sun photometer measurements are valid, but the low variability in E_{sp} (Figure 2c, Table 2) suggests that this may also be the case during other time periods.

[47] The measured values of $\delta_a(\lambda)$ and ω at the surface allow estimation of the direct aerosol radiative forcing (ΔF). Using the method of Haywood and Shine [1995, 1997],

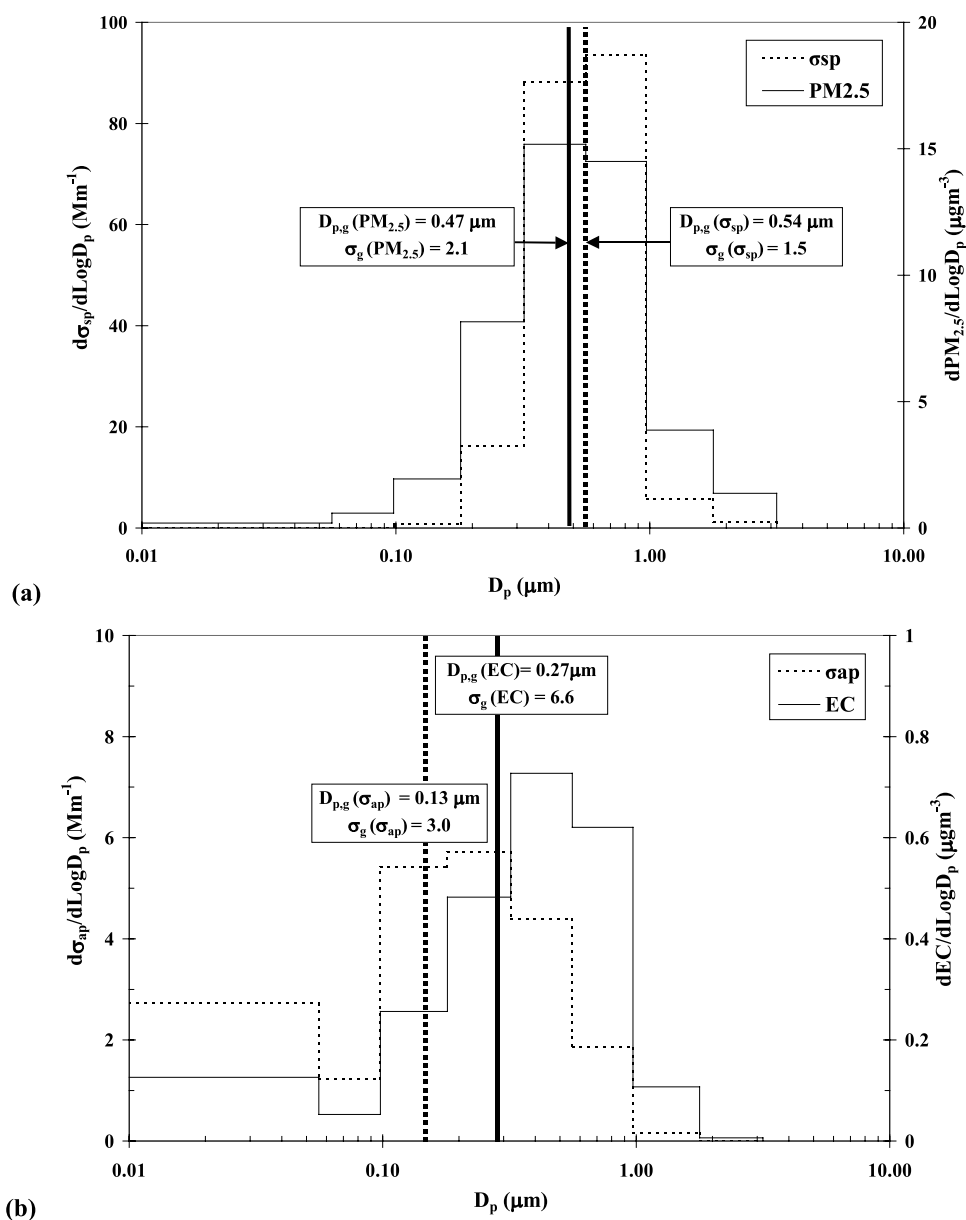


Figure 6. Atlanta Supersite 1999 average (a) MOUDI mass and calculated light scattering distribution (b) MOUDI EC and calculated light absorption distribution.

estimates of ΔF are shown in Figure 8 using the measured aerosol properties $\delta_a(\lambda)$ and ω presented above. As with all the measurements presented here, these ground based measurements assume that the single scattering albedo is constant with height. For these estimates, the calculation is daily averaged with a daylight fraction of 0.5 and assumes a surface reflectivity of $R_s = 0.15$ and a fractional cloud-cover of $A_c = 0.5$ [Charlson *et al.*, 1992]. Also, the upscatter fraction (β) has been attributed values of 0.24 to 0.29 in global scale models [Charlson *et al.*, 1992; Kiehl and Briegleb, 1993], and measurements with a backscatter nephelometer give an estimated upscatter for perturbed aerosol of ~ 0.25 [Ogren, 1995]. For these estimates, β is estimated from the mass size distributions as 0.24. This is on the lower end of the range of estimates stated above and results in a minimum estimate of ΔF . Since measurements

of $\delta_a(\lambda)$ are possible only during cloud-free conditions, a bias in this estimate of ΔF may exist since aerosol concentrations are typically affected near cloudy areas. As is the case with the other extensive optical and physical properties, ΔF shows great variability in time. Estimated average ΔF in Atlanta during the experiment is $-11 \pm 6 \text{ Wm}^{-2}$, a net cooling. The instantaneous ΔF is up to a factor of 4 greater than this assuming daylight, clear-sky conditions. The average direct aerosol radiative forcing estimated here in Atlanta is a cooling effect substantially larger in magnitude than the global mean radiative forcing attributed to anthropogenic aerosol particles (approximately -1 Wm^{-2}) and due to anthropogenic greenhouse gases (approximately $+2.5 \text{ Wm}^{-2}$) [IPCC, 2001]. This indicates a substantial impact of aerosols on radiative transfer in the urban atmosphere of a magnitude having potential implications for

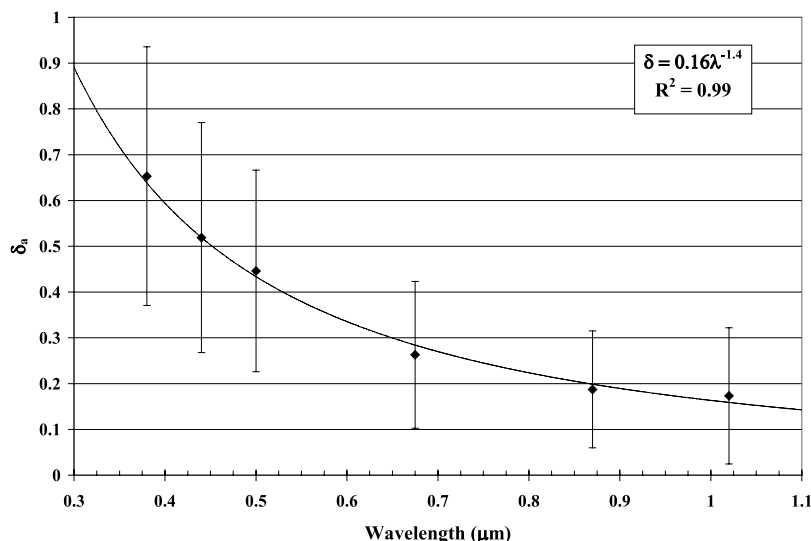


Figure 7. Aerosol optical depth (δ_a) arithmetic means and standard deviations in Atlanta as a function of wavelength of light and best fit power function.

climate, photochemistry, photosynthesis, and atmospheric stability.

4. Conclusions

[48] As part of the Atlanta Supersite 1999 study, $PM_{2.5}$ (particulate material having an aerodynamic diameters $D_p < 2.5 \mu m$) aerosol optical-related properties are investigated in the urban environment. The measurements occurred over ~ 1 month field sampling intensive from 30 July to 3 September 1999 at the Jefferson Street Site in midtown Atlanta, 1.5 km northwest of downtown and within the urban core of Atlanta. Arithmetic means and standard deviations of the midvisible light scattering (σ_{sp} at 530 nm) and absorption coefficients (σ_{ap} at 550 nm) at RH = 49

$\pm 5\%$ are 121 ± 48 and $16 \pm 12 Mm^{-1}$, respectively. The light extinction coefficient (σ_{ep}) is a factor of 2 to 3 higher than typical nonurban polluted sites. Though aerosol optical properties are dominated by light scattering by particles, an estimated single scatter albedo (ω_0) of 0.87 ± 0.08 in Atlanta is lower than nonurban sites due to the influence of local emissions of soot, most likely from mobile sources.

[49] Variability in extensive parameters was related to variability in source strength, air mass transport, atmospheric stability, and aerosol removal mechanisms. A pronounced diel pattern in aerosol radiative properties is observed with clear influences from vehicular traffic (rush hour peaks in concentrations, particularly EC and σ_{ap}) and atmospheric mixing (afternoon troughs). Likewise, a strong influence of meteorology and particularly precipitation

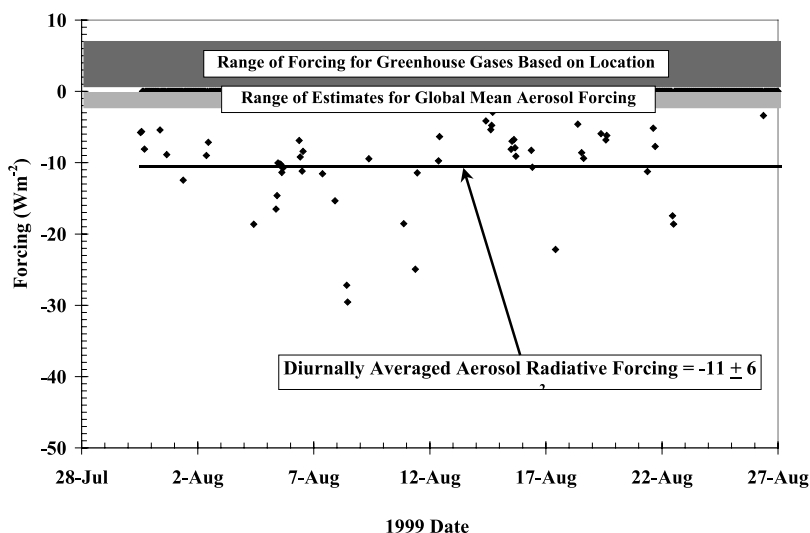


Figure 8. Estimated direct aerosol radiative forcing during the Atlanta Supersite 1999 study based on measurements of aerosol optical depth and single scatter albedo. Calculations are 24 h averaged using the *Haywood and Shine* [1995, 1997] model. The calculation assumes upscatter fraction of 0.24 from past measurements and a cloud cover fraction of $A_c = 0.5$ and a surface reflectivity of $R_s = 0.15$.

events on aerosol optical properties is observed. $PM_{2.5}$ concentrations and σ_{sp} decrease by 50% or more and over the course of several hours during precipitation events, even relatively light events. However, the EC concentration and hence σ_{ap} are less strongly or quickly affected by precipitation, and this results in decreases in ω_0 during precipitation events. This also underscores the importance of aerosol solubility in atmospheric lifetime.

[50] Based on several techniques, a strongly linear relationship is found between $PM_{2.5}$ and σ_{sp} ($R^2 = 0.80$ to 0.96). Similarly, elemental carbon (EC) and σ_{ap} are correlated, though less strongly ($R^2 = 0.34$ to 0.97) while little relationship between σ_{ap} and overall $PM_{2.5}$ exists ($R^2 = 0.19$). This demonstrates that light scattering is dependent on a wide range of chemical components while light absorption is most strongly linked to EC. The mass scattering efficiency of $PM_{2.5}$ is observed to be 3.5 to $4.4 \text{ m}^2 \text{ g}^{-1}$ based on a real-time and two time-integrated mass measurements, and this is very similar to values found in other polluted locations. Spanning the wide range found in other studies, several methods for EC measurements give light absorption efficiencies E_{ap} ranging from 5.3 to $18.3 \text{ m}^2 \text{ g}^{-1}$. Best agreement was found from two techniques using multistage impactor measurements of EC mass size distribution, Mie calculations and measured σ_{ap} giving $E_{ap} = 9.3\text{--}9.5 \text{ m}^2 \text{ g}^{-1}$. Though variable aerosol properties and uncertainty in the light absorption measurement contribute, the determination of E_{ap} is observed in this study to be very dependent on the method of EC determination.

[51] Mie light extinction calculations using inputs of measured mass and EC size distributions show geometric mean light scattering and absorbing diameters to be 0.54 and $0.13 \text{ }\mu\text{m}$ with geometric standard deviations of 1.5 and 3, respectively. This compares to the $PM_{2.5}$ mass and EC geometric mean diameters of 0.47 and $0.27 \text{ }\mu\text{m}$, with geometric standard deviations of 2 and 6.6, respectively. Thus light scattering distribution is predominated by a rather narrow mode of particles in the accumulation mode with $0.1 < D_p < 1 \text{ }\mu\text{m}$ while the EC mass and absorption is relatively more broadly distributed although shifted toward smaller particles.

[52] Measured aerosol optical depth has an average value of $\delta_a(500\text{nm}) = 0.44 \pm 0.22$ and is a strong function of wavelength of light due to the dominant optical influence of submicrometer particles. An exponential curve-fit to $\delta_a(\lambda)$ measurements gives Ångström parameters $\alpha = 1.5 \pm 0.3$ and $\beta = 0.15 \pm 0.07$ and a curve fit parameter of $R^2 = 0.97 \pm 0.06$. Measurements of $PM_{2.5}$ concentration with a real-time method give an average of $31 \pm 12 \text{ }\mu\text{g m}^{-3}$ during the Supersite 1999 experiment. Though this is strictly a summertime measurement during the peak season over a one-month period, it is a factor of two higher than the proposed NAAQS annual standard of $15 \text{ }\mu\text{g m}^{-3}$. Based on these measurements, a rough estimate of the average direct aerosol radiative forcing (a measure of the climate significance) is $-11 \pm 6 \text{ Wm}^{-2}$ in the metro Atlanta area. Compared to the magnitude of global average model estimates of radiative forcing, this is a cooling effect that is roughly an order of magnitude larger than global average due to anthropogenic aerosols and a factor of five greater than the combined forcing of all anthropogenic greenhouse gases. The aerosol radiative forcing varies greatly in time as

a result of the large variability in aerosol properties and particularly $\delta_a(\lambda)$. In addition to the implications for human health and compliance with proposed $PM_{2.5}$ standards, aerosol radiative effects are much larger in the Atlanta metro area than in average nonurban sites. This in turn has implications for climate, visibility, and photochemistry of the urban environment.

[53] **Acknowledgments.** The authors would like to acknowledge the U.S. EPA for supporting this work and Eric Edgerton of ARA, Inc. for the real-time EC and OC measurements. The authors also acknowledge the comments of two anonymous reviewers that have greatly enhanced this work.

References

- Allen, G., C. Sioutas, P. Koutrakis, R. Reiss, F. W. Lurmann, and P. T. Roberts, Evaluation of the TEOM method for measurement of ambient particulate mass in urban areas, *J. Air Waste Manage. Assoc.*, **47**, 682–689, 1997.
- Anderson, T. L., and J. A. Ogren, Determining aerosol radiative properties using the TSI 3563 integrating nephelometer, *Aerosol Sci. Technol.*, **29**, 57–69, 1998.
- Andrews, E., and S. M. Larson, Effect of surfactant layers on the size changes of aerosol particles as a function of relative humidity, *Environ. Sci. Technol.*, **27**, 857–865, 1993.
- Ångström, A., Parameters of atmospheric turbidity, *Tellus*, **16**, 64–75, 1964.
- Ayers, G. P., M. D. Keywood, and J. L. Gras, TEOM vs. manual gravimetric methods for determination of $PM_{2.5}$ aerosol mass concentrations, *Atmos. Environ.*, **33**, 3717–3721, 1999.
- Bergin, M. H., J. A. Ogren, S. E. Schwartz, and L. M. McInnes, Evaporation of ammonium nitrate aerosol in a heated nephelometer: Implications for field measurements, *Environ. Sci. Technol.*, **31**, 2878–2883, 1997.
- Bergin, M. H., et al., Aerosol radiative, physical, and chemical properties in Beijing during June 1999, *J. Geophys. Res.*, **106**, 17,969–17,980, 2001.
- Birch, R. E., and R. A. Cary, Elemental carbon-based method for monitoring occupational exposures to particulate diesel exhaust, *Aerosol Sci. Technol.*, **25**, 221–241, 1996.
- Bohren, C. F., and D. R. Huffman, *Absorption and Scattering of Light by Small Particles*, 530 pp., John Wiley, New York, 1983.
- Bond, T. C., T. L. Anderson, and D. Campbell, Calibration and intercomparison of filter based measurements of visible light absorption by aerosols, *Aerosol Sci. Technol.*, **30**, 582–600, 1999.
- Butler, A. J., Temporal and spatial assessment of $PM_{2.5}$ mass and composition in Atlanta, Ph.D. dissertation, Ga. Inst. of Technol., Atlanta, Ga., 2000.
- Butler, A. J., M. S. Andrew, and A. G. Russell, Daily sampling of $PM_{2.5}$ in Atlanta: Results of the first year of the Assessment of Spatial Aerosol Composition in Atlanta study, *J. Geophys. Res.*, **108**, doi:10.1029/2002JD002234, in press, 2003.
- Carrico, C. M., M. J. Rood, and J. A. Ogren, Aerosol light scattering properties at Cape Grim, Tasmania, during the First Aerosol Characterization Experiment (ACE 1), *J. Geophys. Res.*, **103**, 16,565–16,574, 1998.
- Carrico, C. M., M. J. Rood, J. A. Ogren, C. Neusüß, A. Wiedensohler, and J. Heintzenberg, Aerosol optical properties at Sagres, Portugal, during ACE 2, *Tellus, Ser. B*, **52**, 694–716, 2000.
- Chameides, W. L., et al., Case study of the effects of atmospheric aerosols and regional haze on agriculture: An opportunity to enhance crop yields in China through emission controls?, *Proc. Nat. Acad. Sci.*, **96**(24), 13,626–13,633, 1999.
- Chang, J. S., R. A. Brost, S. A. Isaksen, S. Madronich, P. Middleton, W. R. Stockwell, and C. J. Walcek, A three-dimensional eulerian acid deposition model: Physical concepts and formulation, *J. Geophys. Res.*, **104**, 14,681–14,700, 1987.
- Charlson, R. J., S. E. Schwartz, J. M. Hales, R. D. Cess, J. A. Coakley Jr., J. E. Hansen, and D. J. Hofmann, Climate forcing by anthropogenic aerosols, *Science*, **255**, 423–430, 1992.
- Chow, J. C., J. G. Watson, L. C. Pritchett, W. R. Pierson, C. A. Frazier, and R. G. Purcell, The DRI thermal/optical reflectance carbon analysis system: Description, evaluation and applications in U.S. air quality studies, *Atmos. Environ., Part A*, **27**, 1185–1201, 1993.
- Chow, J. C., J. G. Watson, D. Crow, H. Lowenthal, and T. Merrifield, Comparison of IMPROVE and NIOSH carbon measurements, *Aerosol Sci. Technol.*, **34**, 23–34, 2001.
- Clarke, A. D., Aerosol light absorption by soot in remote environments, *Aerosol Sci. Technol.*, **10**, 161–171, 1989.

- Clarke, A. D., P. K. Quinn, and J. A. Ogren, The INDOEX aerosol: A comparison and summary of chemical, microphysical and optical properties observed from land, ship, and aircraft, *J. Geophys. Res.*, 107(D19), 8033, doi:10.1029/2001JD000572, 2002.
- Coakley, J. A., and P. Chylek, 2-stream approximation in radiative transfer: Including angle of incident radiation, *J. Atmos. Sci.*, 32(2), 409–418, 1975.
- Cohan, D. S., J. Xu, R. Greenwald, M. H. Bergin, and W. L. Chameides, Impact of atmospheric aerosol light scattering and absorption on terrestrial net primary productivity, *Global Biogeochem. Cycles*, 16(4), 1090, doi:10.1029/2001GB001441, 2002.
- Covert, D. S., A. P. Waggoner, R. E. Weiss, N. C. Ahlquist, and R. J. Charlson, Atmospheric aerosols, humidity and visibility, in *Character and Origin of Smog Aerosols*, pp. 559–581, John Wiley, New York, 1979.
- Delene, D., E. Andrews, D. Jackson, A. Jefferson, J. Ogren, P. Sheridan, and J. Wendell, Aerosols and radiation, in *Climate Monitoring and Diagnostics Laboratory Summary, Rep. 25 1998–1999*, edited by R. C. Schnell, D. B. King, and R. M. Rosen, chap. 3, pp. 47–74, U.S. Dep. of Commerce, Nat. Oceanic and Atmos. Admin., Silver Spring, Md., 2001.
- Dickerson, R. R., et al., Thunderstorms: An important mechanism in the transport of air pollutants, *Science*, 235, 460–464, 1997.
- Dickerson, R. R., S. Kondragunta, G. Stenchikov, K. L. Civerolo, B. G. Doddridge, and B. N. Holben, The impact of aerosols on solar ultraviolet radiation and photochemical smog, *Science*, 278, 827–830, 1997.
- Dougle, P. G., and H. M. ten Brink, Evaporative losses of ammonium nitrate in nephelometry and impactor measurements, *J. Aerosol Sci.*, 27, S511–S512, 1996.
- Dzubay, T. G., R. K. Stevens, and C. W. Lewis, Visibility and aerosol composition in Houston, Texas, *Environ. Sci. Technol.*, 16, 514–525, 1982.
- Edgerton, E. S., B. E. Hartsell, J. J. Jansen, J. St. John, and K. Baumann, Chemical and meteorological characteristics of the Jefferson Street monitoring site, *Eos Trans. AGU*, 81(48), Fall Meet. Suppl., abstract A11B-02, 2000.
- Griffing, G. W., Relationships between the prevailing visibility, nephelometer scattering coefficient, and Sun photometer turbidity coefficient, *Atmos. Environ.*, 14, 577–584, 1980.
- Groblicki, P. J., G. T. Wolff, and R. J. Countess, Visibility reducing species in the Denver “brown cloud,” I, Relationships between extinction and chemical composition, *Atmos. Environ.*, 15, 2473–2484, 1981.
- Gundel, L. A., and D. A. Lane, Sorbent-coated diffusion denuders for direct measurement of gas/particle partitioning by semivolatile organic compounds, in *Gas and Particle Phase Measurements of Atmospheric Organic Compounds*, edited by D. A. Lane, pp. 287–332, Gordon and Breach, Amsterdam, 1999.
- Haywood, J. M., and K. P. Shine, The effect of anthropogenic sulfate and soot aerosol on the clear sky planetary radiation budget, *Geophys. Res. Lett.*, 22, 603–606, 1995.
- Haywood, J. M., and K. P. Shine, Multi-spectral calculations of the direct radiative forcing of tropospheric sulphate and soot aerosols using a column model, *Q. J. R. Meteorol. Soc.*, 123, 1907–1930, 1997.
- Hinds, W. C., *Aerosol Technology: Properties, Behavior, and Measurement of Airborne Particles*, John Wiley, New York, 1999.
- Horvath, H., Atmospheric light absorption—A review, *Atmos. Environ., Part A*, 27, 293–317, 1993.
- Horvath, H., Size segregated light absorption coefficient of the atmospheric aerosol, *Atmos. Environ.*, 29, 875–883, 1995.
- Husar, R. B., and W. E. Wilson, Haze and sulfur emission trends in the eastern United States, *Environ. Sci. Technol.*, 27, 12–16, 1993.
- Intergovernmental Panel on Climate Change, *Climate Change 2001: The Scientific Basis, Contribution of Working Group I to the Third Assessment Report of the Intergovernmental Panel on Climate Change*, edited by D. L. Albritton et al., Cambridge Univ. Press, New York, 2001.
- Jacobson, M. Z., Development and application of a new air pollution modeling system, III, Aerosol-phase simulations, *Atmos. Environ.*, 31, 587–608, 1997.
- Kiehl, J. T., and B. P. Briegleb, The relative roles of sulfate aerosols and greenhouse gases in climate forcing, *Science*, 260, 311–314, 1993.
- Koloutsou-Vakakis, S., C. M. Carrico, P. Kus, M. J. Rood, Z. Li, R. Shrestha, J. A. Ogren, J. C. Chow, and J. G. Watson, Aerosol properties at a midlatitude Northern Hemisphere continental site, *J. Geophys. Res.*, 106, 3019–3032, 2001.
- Liousse, C., H. Cachier, and S. G. Jennings, Optical and thermal measurements of black carbon content in different environments: Variation in the specific attenuation cross section sigma (σ), *Atmos. Environ., Part A*, 27, 1203–1211, 1993.
- Malm, W. C., J. F. Sisler, D. Huffman, R. A. Eldred, and T. A. Cahill, Spatial and seasonal trends in particle concentration and optical extinction in the United States, *J. Geophys. Res.*, 99, 1347–1370, 1994.
- Malm, W. C., et al., Spatial and seasonal patterns and temporal variability of haze and its constituents in the United States, *Rep. III*, Coop. Inst. for Res. in the Atmos., Colo. State Univ., Ft. Collins, Colo., 2000.
- Marple, V. A., K. L. Rubow, and S. M. Behm, A microorifice uniform deposit impactor (MOUDI): Description, calibration and use, *Aerosol Sci. Technol.*, 14, 434–446, 1991.
- McMurry, P. H., and X. Q. Zhang, Size distributions of ambient organic and elemental carbon, *Aerosol Sci. Technol.*, 10, 430–437, 1989.
- McMurry, P. H., X. Wang, K. Park, and K. Ehara, The relationship between mass and mobility for atmospheric particles: A new technique for measuring particle density, *Aerosol Sci. Technol.*, 36, 227–238, 2002.
- Meyer, M. B., H. Patashnick, J. L. Ambs, and E. Rupprecht, Development of a sample equilibration system for the TEOM continuous PM monitor, *J. Air Waste Manage. Assoc.*, 50(8), 1345–1349, 2002.
- Mézáros, E., A. Molnar, and J. Ogren, Scattering and absorption coefficients vs. chemical composition of fine atmospheric aerosol particles under regional conditions in Hungary, *J. Aerosol Sci.*, 29(10), 1171–1178, 1998.
- Noone, K. J., J. A. Ogren, A. Hallberg, H.-C. Hansson, A. Wiedensohler, and E. Swietlicki, A statistical examination of the chemical differences between interstitial and scavenged aerosols, *Tellus, Ser. B*, 44, 581–592, 1992.
- Ogren, J. A., A systematic approach to in-situ observations of aerosol properties, in *Aerosol Forcing of Climate*, edited by J. Heintzenberg and R. J. Charlson, pp. 215–226, John Wiley, New York, 1995.
- Okrent, D. A., Optimization of a third generation TEOM monitor for measuring diesel particulate in real-time, *Proc. Soc. Automotive Eng. Pap. 980409*, pp. 209–214, 1998.
- Parkhurst, W. J., R. L. Tanner, F. P. Weatherford, R. J. Valente, and J. F. Meagher, Historic PM_{2.5}/PM₁₀ concentrations in the southeastern United States—Potential implications of the revised particulate matter standard, *J. Air Waste Manage. Assoc.*, 49, 1060–1067, 1999.
- Patashnick, H., and E. G. Rupprecht, Continuous PM-10 measurements using the tapered element oscillating microbalance, *J. Air Waste Manage. Assoc.*, 41, 1079–1083, 1991.
- Penner, J. E., *Carbonaceous Aerosols Influencing Atmospheric Radiation: Black and Organic Carbon*, edited by J. Heintzenberg and R. J. Charlson, pp. 91–108, John Wiley, New York, 1995.
- Penner, J. E., R. J. Charlson, J. M. Hales, N. S. Laulainen, R. Leifer, T. Novakov, J. Ogren, L. F. Radke, S. E. Schwartz, and L. Travis, Quantifying and minimizing uncertainty of climate forcing by anthropogenic aerosols, *Bull. Am. Meteorol. Soc.*, 75(3), 375–400, 1994.
- Reddy, P. J., F. W. Kreiner, J. J. DeLuisi, and Y. Kim, Aerosol optical depths over the Atlantic derived from shipboard Sun photometer observations during the 1988 Global Change Expedition, *Global Biogeochem. Cycles*, 4, 225–240, 1990.
- Ross, C., P. Stevens, and R. Guensler, Spatial and statistical analysis of commercial vehicle activity in metropolitan Atlanta, *Transport. Res. Record* 1625, pp. 165–172, Trans. Res. Board, Washington, D. C., 1998.
- Rupprecht, P., H. Patashnick, D. E. Beeson, R. N. Green, and M. B. Meyer, A new automated monitor for the measurement of particulate carbon in the atmosphere, in *Proceedings, Particulate Matter: Health and Regulatory Issues*, edited by J. A. Cooper and L. D. Grant, pp. 262–267, Air and Waste Manage. Assoc., Pittsburgh, Penn., 1995.
- Russell, A. G., A. Butler, E. Edgerton, and P. Solomon, Local and regional representativeness of the Jefferson Street site, *Eos Trans. AGU*, 81(48), Fall Meet. Suppl., abstract A11B-03, 2000.
- Russell, P. B., S. A. Kinne, and R. W. Bergstrom, Aerosol climate effects: Local radiative forcing and column closure experiments, *J. Geophys. Res.*, 102, 9397–9407, 1997.
- Russell, P. B., et al., Comparison of aerosol single scattering albedos derived by diverse techniques in two North Atlantic experiments, *J. Atmos. Sci.*, 59(3), 609–619, 2002.
- Schmid, H., et al., Results of the carbon conference international aerosol carbon round robin test stage I, *Atmos. Environ.*, 35, 2111–2121, 2001.
- Schwartz, S. E., The Whitehouse effect, shortwave radiative forcing of climate by anthropogenic aerosols: An overview, *J. Aerosol Sci.*, 3, 359–382, 1996.
- Seinfeld, J. H., and S. N. Pandis, *Atmospheric Chemistry and Physics*, John Wiley, New York, 1998.
- Shaw, G. E., Sun photometry, *Bull. Am. Meteorol. Soc.*, 64, 4–10, 1983.
- Stein, S. W., B. J. Turpin, X. Cai, P.-F. Huang, and P. H. McMurry, Measurements of relative humidity dependent bounce and density for atmospheric particles using the DMA-impactor technique, *Atmos. Environ.*, 28, 1739–1746, 1994.
- Tang, I. N., Chemical and size effects of hygroscopic aerosols on light scattering coefficients, *J. Geophys. Res.*, 101, 19,245–19,250, 1996.
- Tang, I. N., Thermodynamic and optical properties of mixed salt aerosols of atmospheric importance, *J. Geophys. Res.*, 102, 1883–1893, 1997.

- Tegen, I., A. A. Lacis, and I. Fung, The influence on climate forcing of mineral aerosols from disturbed soils, *Nature*, *381*, 681–683, 1996.
- Thekaekara, M. P., Solar energy outside the Earth's atmosphere, *Sol. Energy*, *14*, 109–127, 1973.
- Turpin, B. J., and J. J. Huntzicker, Secondary formation of organic aerosol in the Los Angeles basin: Descriptive analysis of organic and elemental carbon concentrations, *Atmos. Environ., Part A*, *25*, 207–215, 1991.
- Turpin, B. J., P. Saxena, and E. Andrews, Measuring and simulating particulate organics in the atmosphere: Problems and prospects, *Atmos. Environ.*, *34*, 2983–3013, 2000.
- Waggoner, A. P., R. E. Weiss, N. C. Ahlquist, D. S. Covert, S. Will, and R. J. Charlson, Optical characteristics of atmospheric aerosols, *Atmos. Environ.*, *15*, 1891–1909, 1981.
- Waggoner, A. P., R. E. Weiss, and T. V. Larson, In-situ, rapid response measurement of $\text{H}_2\text{SO}_4/(\text{NH}_4)_2\text{SO}_4$ aerosols in urban Houston: A comparison with rural Virginia, *Atmos. Environ.*, *17*, 1723–1731, 1983.
- Weber, R. W., et al., Short-term temporal variation in PM_{2.5} mass and chemical composition during the Atlanta Supersite Experiment, 1999, *J. Air Waste Manage. Assoc.*, in press, 2003a.
- Weber, R. J., et al., Intercomparison of near real-time monitors of PM_{2.5} nitrate and sulfate at the Environmental Protection Agency Atlanta Supersite, *J. Geophys. Res.*, *108*, doi:10.1029/2001JD001220, in press, 2003b.
- Wilson, W. E., and H. H. Suh, Fine particles and coarse particles: Concentration relationships relevant to epidemiologic studies, *J. Air Waste Manage. Assoc.*, *47*, 1238–1249, 1997.
- Xu, J., M. H. Bergin, X. Yu, G. Liu, J. Zhao, C. M. Carrico, and K. Baumann, Measurement of aerosol chemical, physical and radiative properties in the Yangtze Delta region of China, *Atmos. Environ.*, *36*, 161–173, 2002.
- Yu, S., C. S. Zender, and V. K. Saxena, Direct radiative forcing and atmospheric absorption by boundary layer aerosols in the southeastern US: Model estimates on the basis of new observations, *Atmos. Environ.*, *35*, 3967–3977, 2001.
-
- K. Baumann, School of Earth and Atmospheric Sciences, Georgia Institute of Technology, 221 Bobby Dodd Way, Atlanta, GA 30332-0340, USA.
- M. H. Bergin and J. Xu, School of Civil and Environmental Engineering, Georgia Institute of Technology, 200 Bobby Dodd Way, Atlanta, GA 30332-0512, USA.
- C. M. Carrico, Department of Atmospheric Science, Foothills Research Campus, Colorado State University, Fort Collins, CO 80523-1371, USA. (carrico@lamar.colostate.edu)
- H. Maring, Rosenstiel School of Marine and Atmospheric Science, University of Miami, 4600 Rickenbacker Causeway, Miami, FL 33149-1098, USA.